

Dear Dr. Pusede

Thank you for providing the last comments on our manuscript, “**Observed trends in ground-level O<sub>3</sub> in Monterrey, Mexico during 1993-2014: Comparison with Mexico City and Guadalajara**”.

We also thank to the helpful comments of all the referees during the revision process. We hope that you will now consider it suitable for publication at ACP.

Please find below our responses to your comments.

**1. The abstract is not well focused. It should be streamlined, conveying just the key summary information.**

**Response:** As requested, the abstract has been streamlined to convey only a summary of results. Text modified: "Here, we present an assessment of long-term trends in O<sub>3</sub> and odd oxygen (O<sub>3</sub> + NO<sub>2</sub>) at the industrial Monterrey metropolitan area (MMA) in NE Mexico. Diurnal amplitudes in O<sub>x</sub> (AV<sub>d</sub>) are used as a proxy for net O<sub>3</sub> production, which is influenced by the NO<sub>2</sub> photolysis rate. No significant differences in the AV<sub>d</sub> are observed between weekends and weekdays, although the largest AV<sub>d</sub> are observed at sites downwind of industrial areas. The highest O<sub>3</sub> mixing ratios are observed in spring, with minimum values in winter. The largest annual variations in O<sub>3</sub> are typically observed downwind of the MMA, with the lowest variations generally recorded in highly populated areas and close to industrial areas. A wind sector analysis of mixing ratios of O<sub>3</sub> precursors revealed that the dominant sources of emissions are located in the industrial regions within the MMA and surrounding area. Significant increasing trends in O<sub>3</sub> in spring, summer and autumn are observed depending on site location, with trends in annual averages ranging between 0.19 and 0.33 ppb yr<sup>-1</sup>. Overall, during 1993 to 2014, within the MMA, O<sub>3</sub> has increased at an average rate of 0.22 ppb yr<sup>-1</sup> ( $p < 0.01$ ), which is in marked contrast with the decline of 1.15 ppb yr<sup>-1</sup> ( $p < 0.001$ ) observed in the Mexico City metropolitan area (MCMA) for the same period. No clear trend is observed during 1996 to 2014 within the Guadalajara metropolitan area (GMA)." See lines: 17-30.

**2. Line 56: chemical loss, not photochemical loss.**

**Response:** Sentence has been modified as requested. See line: 46.

**3. Line 136: In sentence - “We show that air mass origin influences strongly the O<sub>3</sub> annual growth rates.” It is not clear what “growth rates” means.**

**Response:** We have replaced growth rates for increases. See line: 126.

**4. Line 285: Revise - “photochemical season.”**

**Response:** As requested, photochemical season has been deleted.

**5. Line 306: Delete sentence - “Diurnal variations in O<sub>3</sub> arise from the balance between its net production and destruction.”**

**Response:** As requested, the sentence has been deleted.

**6. Line 320: Delete sentence - “O<sub>3</sub> and O<sub>x</sub> levels depend strongly on the photochemical processing of NO<sub>x</sub> and VOCs emissions.”**

**Response:** As requested, the sentence has been deleted.

**7.  $AV_d O_x$  may be a proxy for  $PO_3$ , but not  $AV_d O_3$ .**

**Response:** The co-editor is right. We have rephrased the paragraph to describe that only  $AV_{dS}$  can be used as a proxy to assess net  $O_3$  production. Text modified: " $O_x$  amplitude values ( $AV_d$ ) derived from normalised daily cycles were used as a proxy to assess differences in the net  $O_3$  production from site-to-site within the MMA. The normalised daily cycles were constructed by subtracting daily averages from hourly averages. Figure 4 shows normalised  $O_x$  daily cycles. The lowest  $AV_{dS}$  in  $O_x$  occur in winter consistent with reduced SR and low photolysis rates, with the largest values observed in summer. It is clear that during the year, the largest  $AV_{dS}$  are recorded at sites downwind of industrial emission sources, in particular at STA, while the lowest  $AV_{dS}$  are observed at sites upwind. The larger  $AV_{dS}$  at downwind sites are interpreted to indicate higher net  $O_3$  production, derived from the occurrence of photochemical processed air masses from the E sector. The  $AV_{dS}$  at upwind sites are less affected by emissions from the MMA, and especially the industrial area." See lines: 308-316.

**8. The authors are not convincing that "seasonal amplitude values ( $AV_s$ ) provide insight into inter-annual variations in the net  $O_3$  production in response to changes in precursor emissions and meteorology." Low  $O_3$  in winter may be simply  $O_3$  loss to  $NO$ , not low  $PO_3$ . This would be consistent with the later discussion of substantial  $NO_x$  emission reductions in 1994-1996.**

**Response:** We have rephrased the sentence to describe that  $AV_s$  provide insights of inter-annual variations in  $O_3$ . Text modified: "The seasonal amplitude value ( $AV_s$ ) provide insight into inter-annual variations in net  $O_3$  production in response to changes in precursor emissions, meteorology, and  $O_3$  chemistry." See lines: 329-330.

**9. Line 413: "Stephens et al. (2008) suggested that the most plausible explanation for the lack of weekend  $O_3$  effect at MCMA during 1987-2007, is that weekday  $O_3$  production is limited by VOCs and inhibited by  $NO_x$ ." As described, this would cause weekday-weekend  $O_3$  differences.**

**Response:** The paragraph has been rephrased, stating that the most plausible explanation is the simultaneous decrease in both  $NO_x$  and VOCs emissions during weekends, since the sole decrease in  $NO_x$  emissions under VOC-limited conditions would lead to an increase in  $O_3$ , which is not observed. Text modified: "Stephens et al. (2008) suggested that the most plausible explanation for the lack of weekend  $O_3$  effect at MCMA during 1987-2007 is a simultaneous decrease in  $NO_x$  and VOCs emissions during weekends, since the sole decrease in  $NO_x$  emissions under VOC-limited conditions would lead to an increase in  $O_3$  not observed. Similarly, a VOC-limited  $O_3$  production regime was reported for the MMA by Sierra et al. (2013), whereas Kanda et al. (2016) reported that at the GMA the  $O_3$  production lies in the region between VOC- and  $NO_x$ -sensitivity. Therefore, it can be suggested that simultaneous decreases in  $NO_x$  and VOCs emissions during weekends at the GMA and MMA explain the similar behaviour in  $O_3$  and  $O_x$  as at the MCMA. Moreover, a change to a  $NO_x$ -limited  $O_3$  production regime during weekends at the three urban areas seems unlikely, since this would result in lower  $O_3$  levels during weekends, which is not observed at any of the studied urban areas (Torres-Jardon et al., 2009)." See lines: 399-408.

**10. Figure 9: Colors for  $O_x$  and  $O_3$  in MCMA and MMA are difficult to distinguish.**

**Response:** As requested, Fig. 9 has been modified.

**11. Lines 610-618: Delete. No need to compare to cities globally, keep the focus on cities in Mexico.**

**Response:** Deleted, it was there to provide a wider context.

**12. Lines 643-646:** Delete - not relevant.

**Response:** Deleted.

**13. Lines 648-649:** Delete.

**Response:** Deleted.

**14. Line 659:** Replace "It is clear that" with "It has been shown that" and add citations.

**Response:** The sentence has been rephrased and citations have been added. Text modified: It has been shown that O<sub>3</sub> and O<sub>x</sub> decreases within the MCMA have been driven by reductions in NO<sub>x</sub> and VOCs emissions, and that the implemented strategies described in Sect. 4.1 have proved to be effective in controlling primary emissions (ProAire-MCMA, 2011; Jaimes-Palomera et al., 2016)." See lines: 629-631.

**15. Can the authors recommend NO<sub>x</sub> versus VOC control? Or do the authors advocate for both and why?**

**Response:** We have included a statement suggesting VOCs reductions alone, since reductions in NO<sub>x</sub> may increase O<sub>3</sub>. Text modified: "Finally, according to the results presented here, we recommend preferentially reducing VOCs emissions, which may limit O<sub>3</sub> production in response to a decrease in the VOCs/NO<sub>x</sub> ratio. However, simultaneously reducing NO<sub>x</sub> will have added health benefits of less NO<sub>2</sub>." See lines: 641-643.

# 1 Observed trends in ground-level O<sub>3</sub> in Monterrey, Mexico during 1993-2014: Comparison with 2 Mexico City and Guadalajara

3

4 Iván Y. Hernández Paniagua<sup>1,2</sup>, Kevin C. Clemitshaw<sup>3</sup>, and Alberto Mendoza<sup>1,\*</sup>

5

6 <sup>1</sup>Escuela de Ingeniería y Ciencias, Tecnológico de Monterrey, Campus Monterrey, Av.  
7 Eugenio Garza Sada 2501, Monterrey, N.L., México, 64849

8 <sup>2</sup>Centro de Ciencias de la Atmosfera, Universidad Nacional Autónoma de México, Circuito Exterior de  
9 Ciudad Universitaria, Ciudad de México, 04510, México

10 <sup>3</sup>Department of Earth Sciences, Royal Holloway University of London, Egham, Surrey TW20 0EX, UK.

11 \*Corresponding author: mendoza.alberto@itesm.mx

12

## 13 **Keywords**

14 Air quality, emissions inventory, odd oxygen, time series, wind-sector analysis

15

## 16 **Abstract**

17 Here, we present an assessment of long-term trends in O<sub>3</sub> and odd oxygen (O<sub>3</sub> + NO<sub>2</sub>) at the industrial  
18 Monterrey metropolitan area (MMA) in NE Mexico. Diurnal amplitudes in O<sub>x</sub> (AV<sub>d</sub>) are used as a proxy  
19 for net O<sub>3</sub> production, which is influenced by the NO<sub>2</sub> photolysis rate. No significant differences in the  
20 AV<sub>d</sub> are observed between weekends and weekdays, although the largest AV<sub>d</sub> are observed at sites  
21 downwind of industrial areas. The highest O<sub>3</sub> mixing ratios are observed in spring, with minimum values  
22 in winter. The largest annual variations in O<sub>3</sub> are typically observed downwind of the MMA, with the  
23 lowest variations generally recorded in highly populated areas and close to industrial areas. A wind sector  
24 analysis of mixing ratios of O<sub>3</sub> precursors revealed that the dominant sources of emissions are located  
25 in the industrial regions within the MMA and surrounding area. Significant increasing trends in O<sub>3</sub> in  
26 spring, summer and autumn are observed depending on site location, with trends in annual averages  
27 ranging between 0.19 and 0.33 ppb yr<sup>-1</sup>. Overall, during 1993 to 2014, within the MMA, O<sub>3</sub> has increased  
28 at an average rate of 0.22 ppb yr<sup>-1</sup> ( $p < 0.01$ ), which is in marked contrast with the decline of 1.15 ppb yr<sup>-1</sup>  
29 ( $p < 0.001$ ) observed in the Mexico City metropolitan area (MCMA) for the same period. No clear trend  
30 is observed during 1996 to 2014 within the Guadalajara metropolitan area (GMA).

31

## 32 **1. Introduction**

33 O<sub>3</sub> is a secondary air pollutant formed in the troposphere via the photo-oxidation of CO, methane (CH<sub>4</sub>)  
34 and volatile organic compounds (VOCs) in the presence of NO and NO<sub>2</sub> (NO + NO<sub>2</sub> = NO<sub>x</sub>) (Jenkin and  
35 Clemitshaw, 2000). The system of O<sub>3</sub> production is not linear, and is termed NO<sub>x</sub>-limited, when O<sub>3</sub>  
36 production increases in response to increasing NO<sub>x</sub> emissions, and termed VOC-limited when it  
37 responds positively to emissions of VOCs (Monks et al., 2015; Pusede et al., 2015). Tropospheric O<sub>3</sub> is  
38 of concern to policy makers due to its adverse impacts on human health, agricultural crops and

39 vegetation, and also due to its role as a greenhouse gas despite its relatively short lifetime of around  
40  $22.3 \pm 3.0$  days (Stevenson et al., 2006; IPCC, 2013; WHO, 2014; Lelieveld et al., 2015). As the  
41 predominant source of OH, tropospheric  $O_3$  controls the lifetime of  $CH_4$ , CO, VOCs, among many other  
42 air pollutants (Revell et al., 2015). In polluted regions, increased levels of  $O_3$  are prevalent during  
43 seasons with stable high-pressure systems and intense photochemical processing of  $NO_x$  and VOCs  
44 (Dentener et al., 2005; Xu et al., 2008) with downward transport from the stratosphere of lesser  
45 importance (Wang et al., 2012). By contrast, the main removal processes for tropospheric  $O_3$  are  
46 **chemical** loss and dry deposition (Atkinson, 2000; Jenkin and Clemitshaw, 2000).

47

48 Tropospheric  $O_3$  increased in the Northern Hemisphere (NH) during 1950-1980s due to rapid increases  
49 in precursor emissions during the industrialisation and economic growth of Europe and North America  
50 (NA) (Staehelin and Schmid, 1991; Guicherit and Roemer, 2000). Since the 1990s, reductions in  $O_3$   
51 precursor emissions in economically developed countries have resulted in decreases in tropospheric  $O_3$   
52 levels (Schultz and Rast, 2007; Butler et al., 2012; Pusede et al., 2012), however, in some regions,  
53 increases in  $O_3$  have also been reported. For instance, from an analysis of  $O_3$  data from 179 urban sites  
54 over France during 1999-2012, Sicard et al. (2016) reported an increasing trend in the annual averages  
55 of  $0.14 \pm 0.19$  ppb  $yr^{-1}$ , and in the medians of  $0.13 \pm 0.22$  ppb  $yr^{-1}$ , attributed to long-range transport and  
56 reduced  $O_3$  titration by NO due to reductions in local  $NO_x$  emissions. However, Sicard et al. (2016) also  
57 reported during the same period that at 61 rural sites,  $O_3$  decreased in the annual averages by  $0.12 \pm$   
58  $0.21$  ppb  $yr^{-1}$ , and in the medians by  $0.09 \pm 0.22$  ppb  $yr^{-1}$ .

59

60 In the US and Canada,  $O_3$  levels have decreased substantially at different metrics during the last two  
61 decades in response to more stringent emission controls focused on on-road and industrial sources. In  
62 the Greater Area of Toronto from 2000 to 2012,  $O_3$  levels decreased at urban sites by approximately 0.4  
63 %  $yr^{-1}$ , and at sub-urban sites by approximately 1.1 %  $yr^{-1}$ , as a consequence of a reduction in the mid-  
64 day averages of  $NO_2$  of 5.8 - 6.4 %  $yr^{-1}$ , and in the VOC reactivity of 9.3%  $yr^{-1}$  (Pugliese et al., 2014).  
65 Emission estimates suggest an overall national scale decrease during 1980-2008 in US  $NO_x$  and VOCs  
66 emissions of 40 % and 47 %, respectively, with city-to-city variability (EPA, 2009; Xing et al., 2013).  
67 Lefohn et al. (2010) reported that for 12 US major metropolitan areas, the  $O_3$  US EPA exposure metrics  
68 of the annual 2<sup>nd</sup> highest 1-h average, and the annual 4<sup>th</sup> highest daily maximum 8-h average, decreased  
69 during 1980-2008 at 87 % and 71 % of the monitoring sites evaluated, respectively. However, Lefohn et  
70 al. (2010) observed an increase in the lower- and mid- $O_3$  mixing ratios in response to decreased titration  
71 by NO. More recently, Simon et al. (2015) assessed changes in the 1-h average  $O_3$  mixing ratios at  
72 around 1400 sites across the US between 1998-2013, using the 5<sup>th</sup>, 25<sup>th</sup>, 50<sup>th</sup> 75<sup>th</sup> 95<sup>th</sup> percentiles, and  
73 the maximum daily 8-h average. Overall, Simon et al. (2015) observed increases at the lower end of the  
74  $O_3$  data distribution of 0.1-1 ppb  $yr^{-1}$ , mostly in urban and sub-urban areas, whereas  $O_3$  decreased at the  
75 upper end of the data distribution between 1-2 ppb  $yr^{-1}$  at less urbanised areas. Such changes were

76 associated with the implementation of control strategies within the US to abate peak O<sub>3</sub> mixing ratios, as  
77 the NO<sub>x</sub> SIP Call and, tighter point and vehicle emission standards.

78

79 In Mexico, studies of long-term trends in O<sub>3</sub> have focused on the Mexico City Metropolitan Area (MCMA)  
80 (Molina and Molina, 2004; Jaimes et al., 2012; Rodríguez et al., 2016), with reports of a decrease in O<sub>3</sub>  
81 annual averages of ca. 33 % during the last two decades (Parrish et al., 2011; SEDEMA, 2016a). O<sub>3</sub> has  
82 received less consideration at other large metropolitan areas, where Mexican air quality standards are  
83 frequently exceeded (Table 1). Indeed, since 2000, recorded O<sub>3</sub> mixing ratios have exceeded Mexican  
84 official standards for O<sub>3</sub> 1-h average (110 ppb) and 8-h running average (80 ppb) by more than 50 % at  
85 the Guadalajara metropolitan area (GMA, the second most populated city) and at the Monterrey  
86 metropolitan area (MMA, the third most populated city (INE, 2011; SEMARNAT, 2015). To date, only  
87 Benítez-García et al. (2014) have addressed changes in ambient O<sub>3</sub> at the GMA and MMA during 2000-  
88 2011, reporting an increase in O<sub>3</sub> annual averages of around 47 % and 42 %, respectively. However, it  
89 should be noted that the ordinary linear regression analysis used by Benítez-García et al. (2014) may  
90 be biased by extreme values and is therefore not suitable to determine O<sub>3</sub> long-term trends with  
91 significant confidence.

92

93 To improve air quality, the Mexican government has introduced several initiatives to reduce primary  
94 pollutants emissions, with emission estimates reported in the Mexican National Emissions Inventories  
95 (NEI). The NEI suggest that from 1999 to 2008, anthropogenic NO<sub>x</sub> emissions decreased at the MCMA  
96 by 3.8 % yr<sup>-1</sup>, but increased at the GMA and the MMA by 1.9 % yr<sup>-1</sup>, and by 4.0 % yr<sup>-1</sup>, respectively (Fig.  
97 S1) (SEMARNAT, 2006, 2011, 2014). These NEI NO<sub>x</sub> emission estimates agree with the decrease for  
98 the MCMA of 1.7 % yr<sup>-1</sup> in the NO<sub>2</sub> vertical column density during 2005-2014 reported by Duncan et al.  
99 (2016), but disagree for the GMA and the MMA where decreases of 2.7 % yr<sup>-1</sup> and of 0.3 % yr<sup>-1</sup>,  
100 respectively, are reported. Similarly, Boersma et al. (2008) observed that NO<sub>x</sub> emissions over Mexico  
101 derived from NO<sub>2</sub> satellite observations were higher by a factor of 1.5 - 2.5 times than bottom-up emission  
102 estimates, which were lower by 1.6 - 1.8 times than data reported in the NEI 1999-base year. The NEI  
103 anthropogenic VOCs emissions estimates suggest a decrease at the MMA by 0.2 % yr<sup>-1</sup>, but increases  
104 at the MCMA and at the GMA by 2.7 % yr<sup>-1</sup> and by 3.2 % yr<sup>-1</sup>, respectively (Fig. S1) (SEMARNAT, 2006,  
105 2011, 2014). However, as for NO<sub>x</sub>, NEI trends in VOCs disagree with existing reports for average VOCs  
106 decreases within the MCMA (Arriaga-colina et al., 2004; Garzón et al., 2015).

107

108 Local authorities have developed local emission inventories for the MCMA and the MMA, although only  
109 for the MCMA the inventories have been compiled with a frequency of two years since 1996 (SEDEMA,  
110 1999, 2001, 2003, 2004, 2006, 2008, 2010, 2012, 2014, 2016b; SDS, 2015). The accuracy of the MCMA  
111 emission inventories has been also assessed during several field campaigns. For instance, during the  
112 MCMA 2002-2003 campaign, Velasco et al. (2007) observed an overestimation in the 1998 inventory for  
113 VOCs emissions of alkenes and aromatics, but an underestimation in the contribution of some alkanes.

114 By contrast, for the 2002 MCMA inventory, Lei et al. (2007) reported an underestimation in the VOCs  
115 total emissions of around 65 %, based on a simulation of an O<sub>3</sub> episode occurred in 2003 within the  
116 MCMA. Therefore, since these emission estimates are used to predict future air quality, and to design  
117 clean air policies, it is imperative to examine the results of the policies implemented to control emissions  
118 of O<sub>3</sub> precursors.

119  
120 To our knowledge, no previous study has address trends in O<sub>3</sub> and odd oxygen in urban areas of Mexico.  
121 In this study, we describe trends in ground-level O<sub>3</sub> within the MMA, and its response to changes in  
122 precursor emissions during 1993-2014. Long-term and high-frequency measurements of O<sub>3</sub> were  
123 recorded at 5 air quality monitoring stations evenly distributed within the MMA. In order to better assess  
124 photo-chemical production of O<sub>3</sub>, odd oxygen defined as ([O<sub>x</sub>] = [O<sub>3</sub>] + [NO<sub>2</sub>]) was also considered, as  
125 O<sub>3</sub> and NO<sub>2</sub> are rapidly interconverted. Diurnal and annual cycles of O<sub>3</sub> and O<sub>x</sub> are used to interpret net  
126 O<sub>3</sub> production within the MMA. We show that air mass origin influences strongly the O<sub>3</sub> annual **increases**.  
127 The trends in O<sub>3</sub>, O<sub>x</sub> and precursor emissions are compared with those observed within the MCMA and  
128 GMA. Finally, we describe that NEI emission estimates for NO<sub>x</sub> and VOCs disagree in the trend  
129 magnitudes with ground-based NO<sub>x</sub> and VOCs measurements made at the urban areas studied here.

130  
131 This paper is organised as follows: Section 2 presents the data quality and methodology used to derive  
132 the different trends presented. Section 3 describes in detail the O<sub>3</sub> and O<sub>x</sub> diurnal and annual cycles,  
133 and, annual and seasonally averaged trends. Section 4 discusses the origin of the O<sub>3</sub> and O<sub>x</sub> diurnal  
134 variations and trends in the light of changes in precursor emissions. Finally, Section 5 provides some  
135 conclusions regarding the trends observed at the studied urban areas.

136

## 137 **2. Methodology**

### 138 **2.1 Monitoring of O<sub>3</sub> in the Monterrey Metropolitan Area (MMA).**

139 The MMA (25°40'N, 100°20'W) is located around 720 km N of Mexico City, some 230 km S of the US  
140 border in the State of Nuevo Leon (Fig. 1a). It lies at an average altitude of 500 m above sea level (m  
141 asl) and is surrounded by mountains to the S and W, with flat terrain to the NE (Fig. 1b). The MMA is the  
142 largest urban area in Northern Mexico at around 4,030 km<sup>2</sup>, and is the third most populous in the country  
143 with 4.16 million inhabitants, which in 2010, comprised 88 % of the population of Nuevo Leon State  
144 (INEGI, 2010). It is the second most important industrial area in Mexico and has the highest gross  
145 domestic product per capita (Fig. 1c). Although the weather changes rapidly on a daily time-scale, the  
146 climate is semi-arid with an annual average rainfall of 590 mm, and an annual average temperature of  
147 25.0°C with hot summers and mild winters (ProAire-AMM, 2008; SMN, 2016).

148

149 Within the MMA, tropospheric O<sub>3</sub>, 6 additional air pollutants (CO, NO, NO<sub>2</sub>, SO<sub>2</sub>, PM<sub>10</sub>, and PM<sub>2.5</sub>) and 7  
150 meteorological parameters (wind speed (WS), wind direction (WD), temperature (Temp), rainfall, solar  
151 radiation (SR), relative humidity (RH) and pressure) have been monitored continuously, with data

152 summarised as hourly averages, since November 1992 at 5 stations that form part of the Integral  
153 Environmental Monitoring System (SIMA) of the Nuevo Leon State Government (Table 2; SDS, 2016).  
154 From November 1992 to April 2003, and in accordance with EPA, EQOA-0880-047, Thermo  
155 Environmental Inc. (TEI) model 49 UV photometric analysers were used to measure O<sub>3</sub> with stated  
156 precision less than ±2 ppb O<sub>3</sub> and a detection limit of 2 ppb O<sub>3</sub>. Similarly, in accordance with RFNA-1289-  
157 074, TEI model 42 NO-O<sub>3</sub> chemiluminescence detectors were used to measure NO-NO<sub>2</sub>-NO<sub>x</sub> with stated  
158 precision less than ±0.5 ppb NO, and a detection limit of 0.5 ppb NO. In May 2003, replacement TEI  
159 model 49C O<sub>3</sub> and model 42C NO-NO<sub>2</sub>-NO<sub>x</sub> analysers were operated as above, with stated precision  
160 better than ±1 ppb O<sub>3</sub> and ±0.4 ppb NO, respectively, and detection limits of 1 ppb O<sub>3</sub> and 0.4 ppb NO,  
161 respectively. To rule out instrumentation influences on the determined air pollutants trends, long-term  
162 trends based on annual averages were compared with those derived using 3-yr running averages, in  
163 accordance with Parrish et al. (2011) and Akimoto et al. (2015) (Supplementary Information S1.1; Fig.  
164 S2). Calibration, maintenance procedures and quality assurance/quality control (QA/QC) followed  
165 protocols established in the Mexican standards NOM-036-SEMARNAT-1993 and NOM-156-  
166 SEMARNAT-2012. The SIMA dataset has been validated by the Research Division of Air Quality of the  
167 Secretariat of Environment and Natural Resources (SEMARNAT). The monitoring of O<sub>3</sub> and other air  
168 pollutants at the MCMA and the GMA is detailed in the Supplementary Information S1.2-3.

169

## 170 **2.2 NEI data**

171 NEI data for estimated NO<sub>x</sub> and VOCs emissions for the 1999-, 2005- and 2008-base years were  
172 obtained from the SEMARNAT website (<http://sinea.semarnat.gob.mx>). The data comprised emission  
173 sources (mobile, point, area and natural) and air pollutants (NO<sub>x</sub>, VOCs, SO<sub>x</sub>, CO, PM<sub>2.5</sub> and PM<sub>10</sub>), at  
174 national, state and municipality scales. The NEI emission estimates are developed in accordance with  
175 the Manual for the Emission Inventories Program of Mexico (Radian, 2000), which is based on the US  
176 EPA AP-42 emission factors categorisation (EPA, 1995). The emission factors are regionalised for each  
177 Mexican state, based upon on-site measurements and survey information. Updates to the emission  
178 factors have been conducted for each released NEI, although no changes in the methodology were  
179 implemented between the 1999- and 2008-base years. Overall, the mobile emissions were estimated  
180 using the MOBILE6-Mexico model (EPA, 2003). The emissions from point sources were derived using  
181 the annual operation reports submitted to the Environment Ministry. The emissions from area sources  
182 were obtained using the categorisation of Mexican area sources and the regionalised AP-42 emission  
183 factors.

184

185 The MCMA emissions inventories have been developed with a 2-year frequency since 1996, and were  
186 obtained from the MCMA Environment Secretariat website (<http://www.aire.cdmx.gob.mx/>). The  
187 methodology used to construct the MCMA inventories estimates is consistent with that used in the NEI  
188 (SEDEMA, 2016a), which is based on the AP-42 EPA emission factors. However, more speciated  
189 emission factors have been developed in each released version, considering updates in the local



190 industrial activity, survey information and field measurement campaigns. To date, the only significant  
191 change in the methodology is the replacement of the Mobile6-Mexico model with the MOVES model to  
192 obtain the 2014-base year mobile emissions (SEDEMA, 2016b). As for the MCMA inventories, more  
193 speciated emission factors than those contained in the NEI were developed to produce the MMA  
194 emissions inventory 2013-base year (SDS, 2015), although, estimates of mobile emissions were  
195 obtained with the Mobile6-Mexico model (EPA, 2003).

196

### 197 **2.3 Analytical methods**

198 SIMA, SIMAT (Atmospheric Monitoring System of the MCMA) and SIMAJ (Atmospheric Monitoring  
199 System of the GMA) instrumentation recorded O<sub>3</sub> data every minute, which were then validated and  
200 archived as 1-h averages. Total SIMA O<sub>3</sub> data capture by year and site are shown in Fig. S3. Data  
201 capture averaged during 1993-2014 ranged from 82.6 % at GPE to 93.3 % at SNB, with data capture  
202 <50 % during 1998-2000 at GPE, in 1998 at SNN, and in 1999 at OBI. A threshold of 75% data capture  
203 was defined to consider data valid and representative (ProAire-MMA, 2008; Zellweger et al., 2009;  
204 Wilson et al., 2012). All data were processed with hourly averages used to determine daily averages,  
205 which were used to calculate monthly averages, from which yearly averages were obtained.

206

### 207 **2.4 Data analysis methods**

208 The SIMA, SIMAT and SIMAJ O<sub>3</sub> data sets were analysed extensively using the *openair* package v. 1.1-  
209 4 (Carslaw and Ropkins, 2012) for R software v. 3.1.2 (R Core Team, 2013). In this study, the *openair*  
210 functions *windRose*, *timeVariation* and *TheilSen* were used to analyse air pollution data. Briefly, the  
211 *windRose* summarises wind speed and wind direction by a given time-scale, with proportional paddles  
212 representing the percentage of wind occurrence from a certain angle and speed range. The *timeVariation*  
213 function was used to obtain normalised daily cycles by season, and weekly cycles, with the 95 %  
214 confidence intervals in the cycles calculated from bootstrap re-sampling, which accounts for better  
215 estimations for non-normally distributed data (Carslaw, 2015). Finally, long-term trends of air pollutants  
216 at the MCMA, GMA and MMA were computed with the *TheilSen* function, which is based on the non-  
217 parametric Theil-Sen method (Carslaw, 2015; and references therein). The Theil-Sen estimate of the  
218 slope is the median of all slopes calculated for a given *n* number of *x,y* pairs, while the regression  
219 parameters, confidence intervals and statistical significance are determined through bootstrap re-  
220 sampling. It yields accurate confidence intervals despite the data distribution and heteroscedasticity, and  
221 is also resistant to outliers.

222

223 The trends computed with *openair* were contrasted with those calculated using the MAKESENS 1.0  
224 macro (Salmi et al., 2002) as follows. Firstly, the presence of a monotonic trend was tested with the non-  
225 parametric Mann-Kendal test. For the MCMA, GMA and MMA, the available yearly data are *n*>10, hence  
226 positive values in the *Z* parameter correspond to positive trends and vice-versa for negative values of *Z*.  
227 The significance of the estimated trend was tested at  $\alpha=0.001, 0.01, 0.05$  and  $0.1$  using a two-tailed test.

228 Secondly, slopes of linear trends were calculated with the non-parametric Sen's method, which assumes  
229 linear trends, with a  $Q$  slope and a  $B$  intercept. To calculate  $Q$ , first the slopes of all data values were  
230 calculated in pairs, with the Sen's estimator slope as the median of all calculated slopes. Finally,  $100(1-$   
231  $\alpha)$  % two-sided confidence intervals about the slope estimate were obtained based on a normal  
232 distribution. Comparisons of estimated trends from both approaches are shown in the Supplementary  
233 information S1.4 (Fig. S4).

234

235 The  $O_3$  and other air pollutant time-series were decomposed into trend, seasonal and residual  
236 components using the Seasonal-Trend Decomposition technique (STL; Cleveland et al., 1990). STL  
237 consists of two recursive procedures: an inner loop nested inside an outer loop, assuming measurements  
238 of  $x_i$  (independent) and  $y_i$  (dependent) for  $i = 1$  to  $n$ . The seasonal and trend components are updated  
239 once in each pass through the inner loop; each complete run of the inner loop consists of  $n_{(i)}$  such passes.  
240 Each pass of the outer loop consists of the inner loop followed by a computation of the robustness  
241 weights, which are used in the following run of the inner loop to minimise the influence of transient and  
242 aberrant behaviour on the trend and seasonal components. The initial pass of the outer loop is performed  
243 with all robustness weights equal to 1, followed by  $n_{(o)}$  passes of the outer loop. The Kalman Smoother  
244 (KS) was used to provide minimum-variance, unbiased linear estimations of observations and to impute  
245 missing data to satisfy the STL (Reinsel, 1997; Durbin and Koopman, 2012; Carslaw, 2015). Overall,  
246 statistical seasonal auto-regressive and moving averages with annual seasonal components were  
247 employed. Statistical analyses were carried out with SPSS 19.0.

248

249 In order to carry out seasonal analyses of data, seasons were defined according to temperature records  
250 in the NH, as described previously (Hernandez-Paniagua et al., 2015): winter (December-February),  
251 spring (March-May), summer (June-August) and autumn (September-November). Wind-sector analyses  
252 of data were performed by defining 8 wind sectors each of  $45^\circ$  starting from  $0^\circ \pm 22.5^\circ$ . The lower bound  
253 of each sector was established by adding  $0.5^\circ$  to avoid data duplicity. Data were assigned to a calm  
254 sector when wind speed was  $\leq 0.36 \text{ km h}^{-1}$  ( $0.1 \text{ m s}^{-1}$ ). To assess regional transport, air mass back-  
255 trajectories (AMBT) were calculated using the HYSPLIT model v.4 (NOAA Air Resources Laboratory  
256 (ARL); Stein et al., 2015), with the Global NOAA-NCEP/NCAR reanalysis data files on a latitude-  
257 longitude grid of  $2.5^\circ$ , downloaded from the NOAA ARL website  
258 (<http://ready.arl.noaa.gov/HYSPLIT.php>). HYSPLIT frequency plots of 96-h AMBT were constructed for  
259 every 6 h during the year 2014 with an arrival altitude of 100 m above ground level.

260

### 261 **3. Results**

#### 262 **3.1 Wind occurrence at the MMA**

263 The MMA is highly influenced by anti-cyclonic easterly air masses that arrive from the Gulf of Mexico,  
264 especially during spring and summer (Fig. S5). Figure 2 shows the frequency count of 1-h averages of  
265 wind direction by site and season within the MMA during 1993-2014. At all sites, apart from OBI, the

266 predominant wind direction is clearly E, which occurs between 35-58 % of the time depending on season.  
267 Easterly air masses are augmented by emissions from the industrial area E of the MMA, which are  
268 transported across the urban core and prevented from dispersing by the mountains located S-SW of the  
269 MMA. On average, the highest wind speeds are observed during summer at all sites. By contrast, calm  
270 winds of  $\leq 0.36 \text{ km h}^{-1}$  ( $0.1 \text{ m s}^{-1}$ ) occurred less than 2 % of the time at all sites, most frequently in winter,  
271 and least frequently in summer.

272

### 273 **3.2 Time-series in O<sub>3</sub> and O<sub>x</sub> recorded within the MMA during 1993-2014**

274 Within the MMA, the highest O<sub>3</sub> mixing ratios (1-h averages) are typically observed between April-  
275 September, whereas the lowest values are usually recorded between December-January (winter) (Fig.  
276 S6). Table S1 summarises the minimum, maximum, average (mean) and median hourly O<sub>3</sub> mixing ratios  
277 recorded during 1993-2014. The highest O<sub>3</sub> mixing ratios recorded were 186 ppb at GPE in 1997, 146  
278 ppb at SNN in 2004, and 224 ppb at SNB in 2001. At OBI and STA, the highest O<sub>3</sub> mixing ratios were  
279 both recorded on June 2, 1993: 182 ppb at 12:00 CDT at OBI, and 183 ppb at 13:00 CDT at STA, during  
280 the occurrence of E winds. Note that all times below are given in CDT. Annual O<sub>3</sub> averages varied from  
281  $14 \pm 14$  ppb at OBI in 2001 to  $32 \pm 23$  ppb at SNB in 1993, whereas O<sub>3</sub> annual medians ranged from 10  
282 ppb at OBI in 2001 to 28 ppb at SNN in 1993.

283

284 Reaction with O<sub>3</sub> rapidly converts NO to NO<sub>2</sub>, and therefore mixing ratios of odd oxygen ( $\text{O}_x = \text{O}_3 + \text{NO}_2$ )  
285 were calculated to account for O<sub>3</sub> stored as NO<sub>2</sub> for each hour during 1993-2014 at the 5 sites within the  
286 MMA (Table S2; Fig. S7). Minimum values of O<sub>x</sub> ranged from 2 ppb, observed at all sites mostly during  
287 1993-2014 to 13 ppb at OBI in 2007. Maximum values of O<sub>x</sub> ranged from 99 ppb at SNN in 2002, to 330  
288 at OBI in 1993. O<sub>x</sub> annual averages varied from  $23 \pm 17$  ppb at SNN in 2002 to  $51 \pm 27$  ppb at OBI and  
289 at STA in 2001 and 2006, respectively, whereas O<sub>x</sub> annual medians ranged from 21 ppb at SNB and  
290 SNN, in 2001 and 2002, respectively, to 46 ppb at OBI and STA in 2001 and 2006, respectively. It is  
291 clear that the highest O<sub>3</sub> and O<sub>x</sub> mixing ratios were recorded when control of precursor emissions of  
292 VOCs and NO<sub>x</sub> were less stringent than subsequently.

293

### 294 **3.2 Diurnal variations in O<sub>3</sub> and O<sub>x</sub> within the MMA**

295 Here, O<sub>3</sub> diurnal variations were used to assess changes in the net O<sub>3</sub> production. Figure 3 shows daily  
296 profiles by season of O<sub>3</sub>, O<sub>x</sub>, NO, NO<sub>2</sub>, NO<sub>x</sub>, and SR averaged over the 5 sites within the MMA. O<sub>3</sub>  
297 generally dips during the morning rush hour due to titration with NO and mirrors the increase in NO<sub>2</sub>,  
298 which occurs around 07:00 in spring and summer, and around 08:00 in autumn and winter. The 1-h  
299 difference in the O<sub>3</sub> dip derives from the change to daylight saving time during spring and summer. O<sub>3</sub>  
300 generally peaks during the enhanced photochemical period, around 13:00 in spring, 12:00 in summer  
301 (co-incident with SR), and about 14:00 in autumn and winter. Similar profiles are observed for O<sub>3</sub> in all  
302 seasons, being negatively correlated with NO<sub>2</sub> ( $r=0.93$  (winter) to  $r=0.97$  (summer) ( $p<0.05$ )), due to the  
303 rapid photolysis of NO<sub>2</sub>. Diurnal cycles of O<sub>x</sub> behave as O<sub>3</sub>, with lowest values before the morning rush

304 hour and the largest between midday (summer) and 15:00 (winter). During daytime,  $O_x$  and  $O_3$  diurnal  
305 cycles are strongly correlated in all seasons, ranging from  $r=0.97$  in winter to  $r=0.99$  in autumn ( $p<0.05$ ),  
306 which suggests net  $O_3$  production during daytime.

307

308  $O_x$  amplitude values ( $AV_d$ ) derived from normalised daily cycles were used as a proxy to assess  
309 differences in the net  $O_3$  production from site-to-site within the MMA. The normalised daily cycles were  
310 constructed by subtracting daily averages from hourly averages. Figure 4 shows normalised  $O_x$  daily  
311 cycles. The lowest  $AV_d$ s in  $O_x$  occur in winter consistent with reduced SR and low photolysis rates, with  
312 the largest values observed in summer. It is clear that during the year, the largest  $AV_d$ s are recorded at  
313 sites downwind of industrial emission sources, in particular at STA, while the lowest  $AV_d$ s are observed  
314 at sites upwind. The larger  $AV_d$ s at downwind sites are interpreted to indicate higher net  $O_3$  production,  
315 derived from the occurrence of photochemical processed air masses from the E sector. The  $AV_d$ s at  
316 upwind sites are less affected by emissions from the MMA, and especially the industrial area.

317

### 318 3.3. Annual cycles of $O_3$ and $O_x$ within the MMA

319 Annual variations in  $O_3$  and  $O_x$  are correlated positively with the seasonality of temperature, RH and SR  
320 (Camalier et al., 2007; Zheng et al., 2007). Annual averages cycle for those meteorological variables,  $O_3$   
321 and  $O_x$  were constructed by averaging monthly averages for the same month during the studied period.  
322 Figure 5a shows that  $O_3$  exhibits the maxima during spring and minima in winter, with a downward peak  
323 in early autumn, behaviour characteristic of tropospheric  $O_3$  in the NH.  $O_x$  peaks in spring and dips in  
324 summer, although it is evident that  $NO_x$  emissions lead to apparently similar  $O_x$  levels in winter and  
325 spring despite the decrease in  $O_3$  levels. A correlation analysis among monthly averages for both  $O_3$  and  
326  $O_x$  with temperature, rainfall, RH and SR, revealed that the strongest relationship was between  $O_3$  and  
327 SR ( $r= 0.72$ ,  $p<0.001$ ; Fig. 5a), with relationship evident with  $O_x$ .

328

329 The seasonal amplitude value ( $AV_s$ ) provide insight into inter-annual variations in net  $O_3$  production in  
330 response to changes in precursor emissions, meteorology, and  $O_3$  chemistry. The seasonal cycles in  $O_3$   
331 during 1993-2014 were determined by filtering monthly averages with the STL technique (Cleveland et  
332 al., 1990) (Fig. S8).  $O_3$   $AV_s$ s were calculated as the difference peak-to-trough (spring peak). An average  
333  $O_3$   $AV_s$  of  $15.1 \pm 2.97$  ( $1\sigma$ ) ppb was calculated from 1993 to 2014 within the MMA, with the lowest  $O_3$   
334  $AV_s$  of 10.3 ppb determined in 1998, and the largest  $O_3$   $AV_s$  of 19.0 ppb observed in 2014. Figure 5b  
335 shows that  $O_3$   $AV_s$  decreased significantly at all sites between 1993 and 1997-1998, at rates from 0.78  
336 ppb  $O_3$   $yr^{-1}$  at GPE to 2.28 ppb  $O_3$   $yr^{-1}$  at SNN (Fig. 5c).  $O_3$   $AV_s$ s increased constantly ( $p<0.05$ ) at all sites  
337 since 1998, ranging from 0.90 ppb  $O_3$   $yr^{-1}$  at GPE to 0.75 ppb  $O_3$   $yr^{-1}$  at SNN.  $O_x$   $AV_s$ s exhibited no  
338 discernible trends at all sites for the whole studied period, although, SNN show a significant ( $p<0.05$ )  
339 decline during 1993-2001 ( $1.5$  ppb  $yr^{-1}$ ) and at STA show an increase during 2004-2010 ( $1.3$  ppb  $yr^{-1}$ ).  
340 The trends in  $O_x$  follow those observed for  $NO_x$  at SNN and STA during 1993-2014, which indicates that  
341 nearby industrial emissions have a significant contribution on the observed  $O_x$  levels within the MMA.

342

### 343 **3.4. Long-term trends in O<sub>3</sub> and O<sub>x</sub> within the MMA during 1993-2014**

344 Quantifying the absolute changes in ground-level O<sub>3</sub> in response to trends in its precursor emissions is  
345 crucial to evaluate the impacts of air quality control (Parrish et al., 2009; Simon et al., 2015). The growing  
346 economy within the MMA has increased O<sub>3</sub> precursor emissions from point and area sources, due to the  
347 limited emissions control programs (INEGI, 2015; SDS, 2015). Moreover, predominant E-SE winds  
348 throughout the year transports primary pollutants and their oxidised products downwind from the  
349 industrial area, which can offset reductions in emissions from other sources. Here, to characterise  
350 changes in net O<sub>3</sub> production during 1993-2014 within the MMA in response to changes in its precursor  
351 emissions, long-term trends for daytime (06:00-18:00 CDT) O<sub>3</sub> and O<sub>x</sub> measurements were derived by  
352 averaging data in seasonal periods. Seasonal averaging was used to minimise variability inherent in  
353 longer-term averages and the de-seasonalisation process avoids confounding overall trends, especially  
354 when seasons exhibit opposite trends. (Parrish et al., 2009).

355

356 Figure 6 shows seasonal trends in O<sub>3</sub> within the MMA, and Table 3 summarises the parameterisation of  
357 the trends. Significant increases ( $p < 0.1$ ) in O<sub>3</sub> are observed at all sites, apart from STA, in spring and  
358 summer, while in autumn, O<sub>3</sub> increases significantly only at SNN and SNB. The increases in O<sub>3</sub> range  
359 from 0.26 ppb yr<sup>-1</sup> in spring at OBI to 0.47 ppb yr<sup>-1</sup> in summer at SNN. Overall, the lowest O<sub>3</sub> growth rates  
360 are observed at the urban background GPE site, whereas the largest ones are at the industrial SNN site.  
361 It is worth noting that only SNN and OBI exhibit significant increases in autumn, despite a decrease in  
362 the frequency of high wind speeds (>20 km h<sup>-1</sup>). The existence of significant trends at all sites during  
363 spring-summer, except for OBI, is consistent with the downwind transport of industrial emissions and the  
364 high frequency of photochemical processed air masses with NE-S-SE origin, where the industrial area  
365 is located (Fig. S9).

366

367 Seasonal trends in O<sub>x</sub> are shown in Fig. 7, with the parameters of the trends listed in Table 3. Consistent  
368 with the seasonal O<sub>3</sub> trends observed, significant increases ( $p < 0.1$ ) in O<sub>x</sub> within the MMA are determined  
369 in spring at all sites except for STA, and range from 0.02 ppb yr<sup>-1</sup> at OBI to 0.67 ppb yr<sup>-1</sup> at SNB. It is  
370 worth noting that the industrial SNN and SNB sites show significant increases in O<sub>x</sub> in all seasons, with  
371 the lowest growth rates in winter and the largest in summer and spring, respectively. Moreover, STA  
372 exhibits the only significant decrease in O<sub>x</sub> of 0.63 ppb yr<sup>-1</sup> during winter. As for O<sub>3</sub>, the O<sub>x</sub> increasing  
373 trends are consistent with the transport of primary emissions during the high occurrence of NE-E-SE air  
374 masses at WS >10 km h<sup>-1</sup>, which is highlighted during the photochemical season (April-September).  
375 Furthermore, the small shift in wind direction at STA to NW during winter coincides with the only observed  
376 decrease in net O<sub>3</sub> production within the MMA, which confirms that O<sub>3</sub> precursors are emitted E of the  
377 MMA. This also makes evident that increasing upwind industrial emissions have offset reductions in  
378 emissions from on-road sources as revealed by the decline in NO<sub>x</sub> evident at OBI.

379

### 380 **3.5 Comparison of MMA O<sub>3</sub> and O<sub>x</sub> weekly profiles with those at MCMA and GMA**

381 O<sub>3</sub> production varies from city-to-city in response to local NO<sub>x</sub> and VOCs emissions. Assessment of  
382 weekly profiles of O<sub>3</sub> and O<sub>x</sub> may provide insights of the geographic response in net O<sub>3</sub> production to  
383 diurnal variations in precursor emissions. Hourly O<sub>3</sub> and O<sub>x</sub> averages were used to construct weekday  
384 and weekend average profiles for the MCMA from 1993 to 2014, and for the GMA from 1996 to 2014.  
385 Figure 8 compares weekly O<sub>3</sub> and O<sub>x</sub> profiles by season within the MMA with those for the MCMA and  
386 GMA. In each case, and consistent with observations in other major urban areas of NA, the lowest O<sub>3</sub>  
387 mixing ratios occur during the morning rush hour due to O<sub>3</sub> titration with NO emitted from on-road  
388 sources, whereas peak values of O<sub>3</sub> are apparent after mid-day during periods of enhanced SR  
389 (Stephens et al., 2008; Jaimes-Palomera et al., 2016). It should be noted that the peak value of O<sub>3</sub> for  
390 the GMA in winter and spring occurs an hour or so earlier than for the MMA and MCMA, which is  
391 consistent with higher VOC/NO<sub>x</sub> emissions ratios at the GMA (Kanda et al., 2016). As might be  
392 anticipated, larger AV<sub>d</sub> of 76.9 ± 1.6 ppb O<sub>3</sub> are observed for the MCMA than for the GMA (46.1 ± 1.0  
393 ppb O<sub>3</sub>) and MMA (37.6 ± 0.4 ppb O<sub>3</sub>), related to the levels of emissions of the O<sub>3</sub> precursors. The O<sub>x</sub>  
394 profiles show a trough during the morning rush hour and a peak between 12:00 and 14:00 at all urban  
395 areas. Despite large variations between weekday and weekend NO<sub>x</sub> mixing ratios at the 3 urban areas  
396 as shown in Fig. 8, no significant differences (*p*>0.05) in O<sub>3</sub> and O<sub>x</sub> are observed at any of the  
397 metropolitan areas between O<sub>3</sub> and O<sub>x</sub> weekends and weekdays AV<sub>d</sub>s.

398

399 Stephens et al. (2008) suggested that the most plausible explanation for the lack of weekend O<sub>3</sub> effect  
400 at MCMA during 1987-2007 is a simultaneous decrease in NO<sub>x</sub> and VOCs emissions during weekends,  
401 since the sole decrease in NO<sub>x</sub> emissions under VOC-limited conditions would lead to an increase in O<sub>3</sub>  
402 not observed. Similarly, a VOC-limited O<sub>3</sub> production regime was reported for the MMA by Sierra et al.  
403 (2013), whereas Kanda et al. (2016) reported that at the GMA the O<sub>3</sub> production lies in the region  
404 between VOC- and NO<sub>x</sub>-sensitivity. Therefore, it can be suggested that simultaneous decreases in NO<sub>x</sub>  
405 and VOCs emissions during weekends at the GMA and MMA explain the similar behaviour in O<sub>3</sub> and O<sub>x</sub>  
406 as at the MCMA. Moreover, a change to a NO<sub>x</sub>-limited O<sub>3</sub> production regime during weekends at the  
407 three urban areas seems unlikely, since this would result in lower O<sub>3</sub> levels during weekends, which is  
408 not observed at any of the studied urban areas (Torres-Jardon et al., 2009). Wolff et al. (2013) observed  
409 at several urban areas in the US similar O<sub>3</sub> levels during weekdays and weekends despite lower O<sub>3</sub>  
410 precursor emissions over weekends. Furthermore, the number of sites in the US that exhibited a  
411 weekend effect decreased from ca. 35 % to less than 5 % from 1997-1999 to 2008-2010, which was  
412 attributed to an increase in the VOC/NO<sub>x</sub> emission ratio derived from a greater decline in NO<sub>x</sub> than in  
413 VOCs emissions, mostly driven by reductions from on-road sources.

414

### 415 **3.6 Long-term trends at MCMA, GMA and MMA from 1993 to 2014**

416 The high mixing ratios of O<sub>3</sub> observed typically at the 3 largest urban areas in Mexico have motivated  
417 the introduction of control strategies to decrease emissions of the O<sub>3</sub> precursors, NO<sub>x</sub> and VOCs. The

418 success of the control strategies implemented can be evaluated by assessing trends in  $O_3$  and  $O_x$ . As  
419 for the MMA, seasonal trends in  $O_3$  and  $O_x$  within the MCMA and GMA were calculated from daytime  
420 measurements. Figure 9 shows a comparison of inter-annual trends in  $O_3$  and  $O_x$  at the 3 urban areas  
421 in Mexico, and Table 4 lists the parameters of the trends. Overall, during 1993-2014, daytime  $O_3$  at the  
422 MCMA decreased significantly ( $p < 0.05$ ) by  $1.15 \text{ ppb yr}^{-1}$  ( $2.04 \% \text{ yr}^{-1}$ ), and increased at the MMA by  $0.22$   
423  $\text{ppb yr}^{-1}$  ( $0.84 \% \text{ yr}^{-1}$ ); at the GMA no discernible trend was observed during 1996-2014. For daytime  $O_x$   
424 at the MCMA and GMA during the same periods, significant decreases ( $p < 0.05$ ) of  $1.87$  and  $1.46 \text{ ppb yr}^{-1}$   
425 were determined, respectively, while the MMA does not exhibit a significant change. At the MCMA, the  
426 overall trends in  $O_3$  and  $O_x$  are strongly driven by their wintertime decreases of  $1.62$  and  $2.47 \text{ ppb yr}^{-1}$ ,  
427 respectively; whereas at the MMA, the annual growth in  $O_3$  is driven by increases in spring and summer  
428 of  $0.32$  and  $0.27 \text{ ppb yr}^{-1}$ , respectively. Although, at the MMA, an increase in  $O_x$  of  $0.28 \text{ ppb yr}^{-1}$  is  
429 observed only during summer, the overall  $O_x$  trend is strongly affected by the non-significant trends in  
430 the other seasons. It is worth nothing that at the GMA, the overall decrease in  $O_x$  of  $1.46 \text{ ppb yr}^{-1}$  is  
431 similar for all seasons, which range between  $1.40 \text{ ppb yr}^{-1}$  (autumn) and  $1.89 \text{ ppb yr}^{-1}$  (spring).

432  
433 The overall trends in net  $O_3$  production during 1993-2014 at the MCMA and GMA are consistent with the  
434 significant ( $p < 0.05$ ) annual decreases in  $NO_x$  of  $1.21$  and  $1.25 \text{ ppb yr}^{-1}$ , respectively (Fig. 10). By contrast,  
435 while average  $NO_x$  levels have increased annually at the MMA at  $0.33 \text{ ppb yr}^{-1}$  ( $p < 0.05$ ), the average net  
436  $O_3$  production has remain steady. Either the non-linear response in  $O_x$  to the changes in  $NO_x$  in an  
437 environment of high  $NO_x$  mixing ratios ( $> 60 \text{ ppb}$ ) displace the chemical equilibrium to favour NO as the  
438 dominant component of  $NO_x$  which does not account for the levels of  $O_x$  (Clapp and Jenkin, 2001). Or  
439 the  $O_x$  trends derived from the combined data set for the MMA do not represent local observed trends,  
440 because a compensating effect between  $O_x$  reductions and increases.

441

### 442 **3.7 Compliance with the 1-h and 8-h Mexican Standards for $O_3$ within the MMA**

443 Between 1993 and 2014, there were two official standards for maximum permitted mixing ratios of  $O_3$  in  
444 Mexico: i) a running 8-h average of  $80 \text{ ppb}$ , not to be exceeded more than 4 times per calendar year,  
445 and ii) a 1-h average of  $110 \text{ ppb}$  (NOM-020-SSA1-1993). Since 19 Oct 2014, the maximum permitted  $O_3$   
446 levels were lowered to a running 8-h average of  $70 \text{ ppb}$  and a 1-h average of  $95 \text{ ppb}$ , (NOM-020-SSA1-  
447 2014). However, because both standards are applicable for whole calendar years, the old permitted  $O_3$   
448 levels were used in this study to determine the number of annual exceedances to both  $O_3$  standards.  
449 Figure 11 shows that within the MMA, the  $O_3$  1-h average and the running 8-h standards were frequently  
450 exceeded (INE, 2011; SEMARNAT, 2015). The largest number of exceedances occurs at STA, followed  
451 by SNB, GPE and OBI, whereas the fewest breaches are observed at SNN markedly since 2004.  
452 However, there have been 3 periods of clear decreased exceedances at all sites (except STA in 2014),  
453 during 1994-1995, 1999-2000, and 2012-2013, which are consistent with marked changes in the national  
454 GDP during economic recessions in Mexico (Fig. S10a). However, although, national GDP exhibits a

455 notable decrease during the 2008-2009 global economic recession, only in 2009 do the O<sub>3</sub> annual  
456 exceedances within the MMA seem to follow (Fig. S10b).

457  
458 Therefore, if O<sub>3</sub> levels continue to increase within the MMA, as determined in the long-term trend  
459 assessment, an increase also in peak O<sub>3</sub> mixing ratios is likely to occur. Hence, to analyse changes in  
460 peak O<sub>3</sub>, daily maxima 1-h averages from 1993 to 2014 were used to determine seasonal trends in peak  
461 levels. Figure 12 shows trends in 1-h daily maxima and Table 5 list the parameters of the trends. Daily  
462 maxima O<sub>3</sub> 1-h averages have increased significantly ( $p < 0.05$ ) in spring and summer at all sites, except  
463 for STA, and also in autumn at the industrial sites SNN and SNB. The largest increases in the daily  
464 maxima are seen at SNN, where similar increases between 0.85 and 0.93 ppb yr<sup>-1</sup> are determined  
465 between spring and autumn. SNB exhibits slightly lower growth rates in spring and summer, but a large  
466 difference in autumn. We have shown that predominantly E-SE winds transport photochemically  
467 processed air masses to SNN and SNB during spring-summer leading to the observed exceedances.  
468 Moreover, the change in the wind occurrence in autumn at SNB leads to a lower growth rate than at  
469 SNN, where the calmest winds during the whole year drive the largest increase interpreted to be due to  
470 the photochemical processing of precursors emitted locally. The GPE and OBI sites exhibit increases  
471 only in spring and summer, with the lowest increases of all sites determined at OBI of 0.48 ppb yr<sup>-1</sup> in  
472 spring, which contrasts with the largest increase at OBI during the same season. However, such  
473 increases are consistent with an increase in the occurrence of NE and E air masses at high speeds (>10  
474 km h<sup>-1</sup>) during spring-summer. STA shows a significant decrease in the maxima daily O<sub>3</sub> 1-h averages  
475 of 0.35 ppb yr<sup>-1</sup> in winter, which is consistent with an increase in the occurrence of NW air masses at WS  
476 < 5 km h<sup>-1</sup>, loaded with high NO<sub>x</sub> mixing ratios (50 ppb) that promote the O<sub>3</sub> titration.

477

## 478 **4. Discussion**

### 479 **4.1 Strategies for air quality control in Mexico**

480 The Mexican environmental authorities have focused largely on improving the air quality within the  
481 MCMA since 1986, by implementing numerous strategies to control primary emissions, but have paid  
482 less attention to other large metropolitan areas in Mexico (PICCA, 1990; ProAire-MCMA, 2011). Control  
483 measures have been designed based on NAEI and local emission inventories data, which possess  
484 significant uncertainties (Arriaga-Colina et al., 2004; Velasco et al., 2007; Kanda et al., 2016). However,  
485 despite these uncertainties, the emission control strategies have helped to reduce O<sub>3</sub> levels within the  
486 MCMA since 1991-1992 (ProAire-MCMA, 2001). Here, we describe the most effective measures  
487 introduced to control O<sub>3</sub> precursor emissions within the MCMA, and then discuss potential benefits of  
488 implementing such measures within the MMA.

489

490 From 1993 to 2014, NO<sub>x</sub> levels within the MCMA decreased at a rate of around 1.2 ppb yr<sup>-1</sup> (1.6 % yr<sup>-1</sup>)  
491 as determined from ground-based measurements. This decline is remarkably consistent with the  
492 decrease during 2005-2014 in the NO<sub>2</sub> column over the MCMA of 1.6 % yr<sup>-1</sup> reported by Duncan et al.



493 (2016). The decrease in NO<sub>x</sub> has been driven largely by reductions in emissions from on-road sources,  
494 in response to the introduction of mandatory 3-way catalytic converters in new vehicles since 1993  
495 (NOM-042; SEMARNAT, 1993), and by the introduction of a no driving day and more stringent exhaust  
496 emissions inspection programs for private cars since 1989 (NOM-041; SEMARNAT, 1993). The NO<sub>x</sub>  
497 reduction measures also required public transport vehicles to switch from petrol to LP gas fuelled  
498 engines, new road corridors were designed for improving the intracity transport and the public transport  
499 fleet was renewed (ProAire-MCMA, 2001). For industrial sources, the switch from fuel oil to LP gas fuel,  
500 relocation of highly polluting industries away from the MCMA, and implementation of regular inspections  
501 programs of NO<sub>x</sub> emission for industrial and area sources were also implemented (ProAire-MCMA,  
502 2001).

503

504 While the outlook for NO<sub>x</sub> levels within the MCMA is clear, studies of VOCs levels have reported no  
505 concluding trends. For instance, Arriaga-Colina et al. (2004) reported a decrease in VOCs of around 10  
506 % from 1992 to 2001 over the N MCMA, while Garzón et al. (2015) reported that on average VOCs  
507 increased over most of the MCMA between 1992-2002 but decreased by 2.4 ppb yr<sup>-1</sup> between 2002-  
508 2012. However, the decrease in VOCs from 2002 to 2012 reported by Garzón et al. (2015) is consistent  
509 with a reduction in light alkanes and aromatics levels during the morning rush hour reported by Jaimes-  
510 Palomera et al. (2016). Continuous measurements of VOCs have been introduced recently by the MCMA  
511 government, which precludes an assessment of VOCs long-term trends. The measures implemented to  
512 control VOCs emissions from on-road sources have included the reformulation of petrol with the  
513 reduction of highly reactive VOCs and addition of oxygenated compounds, and fitting of 3-way catalytic  
514 converter in all new vehicles (NOM-042; SEMARNAT, 1993; ProAire-MCMA, 2001). For area sources,  
515 control measures include the introduction of vapour emissions control systems at petrol stations and  
516 introduction of a LP gas leak detection program for the distribution network (ProAire-MCMA, 2011). As  
517 for NO<sub>x</sub>, industrial VOCs emission sources have been subject to regular emissions inspections and  
518 relocation of the most significant emitters (ProAire-MCMA, 2011).

519

520 Therefore, the moderate success on controlling O<sub>3</sub> levels within the MMA can be interpreted as the  
521 implementation of effective controls measures on VOCs and NO<sub>x</sub> emissions. Thus, a comparison  
522 between VOCs and NO<sub>x</sub> trends derived from the NAEI and local emissions inventories with those  
523 determined from ground-levels measurements can provide insight into further improvements in  
524 decreasing O<sub>3</sub> levels not only within the MCMA but also at other large metropolitan areas in Mexico.  
525 Within the MCMA, the NAEI NO<sub>x</sub> emissions trends are consistent with the decrease determined from  
526 ground-based measurements made by SIMAT, but the MCMA local inventory trends disagree with the  
527 SIMAT trends (Fig. S1 and Fig. 10). For VOCs, the NAEI and the MCMA inventories oppose measured  
528 trends in VOCs during 1993-2001 (Arriaga-Colina et al., 2004; Garzón et al., 2015). This can be  
529 explained by underestimates of VOC emissions within the MCMA of a factor of 2-3 (Arriaga-Colina et al.,

2004; Velasco et al., 2007). Such discrepancies suggest that, significant improvements in NO<sub>x</sub> and VOCs emissions inventories are still required to better inform O<sub>3</sub> control strategies.

532

#### 533 **4.2 Ground-level O<sub>3</sub> and O<sub>x</sub> variations within the MMA**

534 The O<sub>3</sub> and O<sub>x</sub> diurnal variations result from the particular chemical environment and meteorological conditions at each monitoring site within the MMA. Thus, the largest O<sub>3</sub> and O<sub>x</sub> mixing ratios, except for OBI, are observed typically for air masses from the E and SE wind sectors, whereas at OBI, the largest O<sub>3</sub> and O<sub>x</sub> values are recorded during the occurrence of NE and E air masses. It is clear that short-range transport and large upwind emissions of O<sub>3</sub> precursors from the industrial area dominate the MMA (SEMARNAT, 2006, 2011, 2014; SDS, 2015). This is underlined at OBI with the highest values of O<sub>x</sub> where the predominant wind direction is NE, consistent with the transport of emissions from the industrial area located NE, and photochemical processing of air masses (Carrillo-Torres et al., 2017). The daily cycles of O<sub>3</sub> determined within the MMA are consistent with those reported for Los Angeles (VanCuren, 2015), and Toronto (Pugliese et al., 2014). At Toronto, the O<sub>3</sub> maxima were enhanced by the arrival of photochemical processed air masses transported from polluted wind sectors, and decreased during clear air masses. This behaviour is similar to that observed within the MCMA with enhanced O<sub>3</sub> maxima during the occurrence of E-SE (polluted) and decreased levels when SW-W (relatively clean) air masses occurred.

548

#### 549 **4.3. Origin of the O<sub>3</sub> annual cycles within the MMA**

550 The O<sub>3</sub> annual cycles within the MCMA are consistent with the spring maxima and winter minima characteristic of the US southeast regions (Strode et al., 2015), and follow the O<sub>3</sub> cyclic pattern at NH mid-latitudes (Monks 2000; Vingarzan, 2004). However, they are different to O<sub>3</sub> annual cycles reported for the US west coast regions, particularly in California, where the maxima in the cycle occurs between June-August, driven the local influence of precursor emissions upon O<sub>3</sub> production and photochemical conditions (Vingarzan, 2004; Strode et al., 2015). The recurrent downward spikes in the O<sub>3</sub> annual cycles within the MMA between July-August result from high wind speeds (>10 km h<sup>-1</sup> on average) that disperse O<sub>3</sub> precursors and increase the boundary layer height (ProAire-MMA, 2008). The peak in O<sub>3</sub> observed in September is characteristic of humid regions, and can be ascribed to an increase in OH radicals derived from the increment in RH during the rainy season (Lee et al., 2014). A marked increase in RH within the MMA during September is consistent with the increase in O<sub>3</sub> observed as reported by Lee et al. (2014). Over the mid-western and eastern US regions, that O<sub>3</sub> peak has become less noticeable since 2000 (Zheng et al., 2007).

563

564 The annual variability in O<sub>3</sub> within the MMA is strongly coupled to the economic conditions (GDP) in Mexico. For instance, the economic crisis of 1994-1996 caused a marked reduction in industrial emissions of VOCs and NO<sub>x</sub>, which is confirmed by the significantly decrease in O<sub>3</sub> annual variations at all sites within the MMA (Tiwari et al., 2014; INEGI, 2016). During the global economic recession of 2008-

2009, Castellanos and Boersma (2012) reported a reduction of 10-30 % in tropospheric NO<sub>2</sub> over large European urban areas, which is consistent with a faster decline of  $8 \pm 5 \text{ \% yr}^{-1}$  in the NO<sub>2</sub> column density during the same period for US urban regions (Russell et al., 2012). Increases in the NO<sub>2</sub> column density over the MMA as reported by Duncan et al. (2016) are explained by the gradual recovery of the economy since 1997 in Mexico. Moreover, increases in O<sub>3</sub> precursor emissions and in annual variability observed within the MMA are consistent with such economic growth. This explains clearly the opposite trends in O<sub>3</sub> annual variations before and after the economic crisis within the MMA, with the lowest changes seen at the urban GPE site and the greatest ones detected for the SNN industrial site.

#### 4.4 Increasing O<sub>3</sub> and O<sub>x</sub> levels within the MMA

Ground-based measurements made during 1993-2014 reveal significant ( $p < 0.05$ ) increases in NO<sub>x</sub> within the MMA at all sites, apart from OBI, which exhibits a significant decrease (Fig. 13). Overall, the NO<sub>x</sub> increase within the MMA of  $1.24 \text{ \% yr}^{-1}$  ( $0.33 \text{ ppb yr}^{-1}$ ) during 1993-2014 is larger than the increase in the NO<sub>2</sub> column density over the MMA of around  $0.78 \text{ \% yr}^{-1}$  during 2005-2014 reported by Duncan et al. (2016), although both indicate a significant increase in the NO<sub>x</sub> levels at least since 2005. The largest increases in NO<sub>x</sub> correspond to industrial sites, SNN ( $0.51 \text{ ppb yr}^{-1}$ ) and SNB ( $0.74 \text{ ppb yr}^{-1}$ ), which is interpreted as a response to growing industrial activity, in combination with flexible emission regulations within the MMA (INEGI, 2016). The influence of industrial emissions upon O<sub>3</sub> at the MMA becomes evident by the lowest NO<sub>x</sub> growth rate observed at GPE of  $0.19 \text{ ppb yr}^{-1}$ , since OBI has few occurrences of air masses transporting pollutants from the largely industrialised areas throughout the year (Fig. 2). By contrast, the NO<sub>x</sub> decrease at OBI of  $-0.40 \text{ ppb yr}^{-1}$  arises from decreases in emissions from on-road sources (SDS, 2015). The large growth rates in O<sub>3</sub> and NO<sub>x</sub> at SNN and SNB are explained by increasing emissions of O<sub>3</sub> precursors from a growing number of industries and the urban development E of the MMA. The most likely explanation for the O<sub>3</sub> increase at OBI is a reduced titration effect by decreasing NO<sub>x</sub> levels in combination with the non-linear response in O<sub>3</sub> production to decreasing NO<sub>x</sub> emissions under the VOC-sensitive MMA airshed (Sierra et al., 2013; Menchaca-Torre et al. 2015).

The O<sub>x</sub> long-term trends during 1993-2014 within the MMA were consistent with those for O<sub>3</sub> at all sites. Decreases in NO<sub>x</sub> and O<sub>3</sub> observed between 1994-1996 were the response to the economic crisis during the same period in Mexico, when the DGP decreased by 5.9 % providing additional evidence of the dominant role of industries within the MMA. Consistent with economic indicators, annual averaged petrol sales in the Nuevo Leon state in 1995 decreased by 2.4 % in relation to 1994, but increased linearly from 1996 to 2008 at an approximate rate of  $98,800 \text{ m}^3 \text{ petrol yr}^{-1}$  ( $r = 0.90$ ) (Fig. S11) (SENER, 2015). As for petrol sales, registered vehicles in Nuevo Leon show significant variations between 1993-1996, but increase linearly since 1997 at a rate of around  $100,000 \text{ vehicles yr}^{-1}$  ( $r=0.99$ ). This confirms that despite the annual growth in the vehicular fleet, the fitting of 3-way catalyst technology and reformulation of petrol introduced in 1997 has controlled on-road primary emissions (ProAire-MCMA, 2001) The decreases in NO<sub>x</sub> observed at OBI and at all sites during the occurrence of SW-W-NW air masses reflect that if

606 applied, stricter emissions controls such as those for on-road sources can lead to a significant abatement  
607 in primary emissions. It is clear that the industrial sources must be subject to similar emission control  
608 measures as those implemented within the MMA for effectively reducing the O<sub>3</sub> levels.

#### 609 610 **4.5 The opposite O<sub>3</sub> trends at Mexican urban areas**

611 The comparison of O<sub>3</sub> and O<sub>x</sub> trends at MMA, GMA and MCMA reveals different emission trends at each  
612 of the studied cities. The trends in O<sub>3</sub> reported in this study for the MCMA, agree with the reduction of  
613 20 ppb O<sub>3</sub> during 1991-2011 for the MCMA (Jaimes et al., 2012), and with the reduction of 8 ppb O<sub>3</sub>  
614 during 2000-2011 for the MMA (Benítez-García et al., 2014). At the GMA, the no trend status in O<sub>3</sub>  
615 determined here is in contrast with the increase of 12 ppb O<sub>3</sub> during 2000-2011 (Benítez-García et al.,  
616 2014), which is due to the different periods assessed in the latter. Decreases in O<sub>3</sub> in US urban areas  
617 arise from effective control of O<sub>3</sub> precursor emissions (Strode et al., 2015), which has occurred at the  
618 MCMA.

619  
620 Figure 10 shows that NO<sub>x</sub> decreased significantly within the MCMA (1.57 % yr<sup>-1</sup>) and the GMA (1.83 %  
621 yr<sup>-1</sup>) during 1993-2014 and 1996-2014, respectively, but increased within the MMA (1.83 % yr<sup>-1</sup>) during  
622 1993-2014. Such NO<sub>x</sub> trends are within the range of the trends in the NO<sub>2</sub> column density reported by  
623 Duncan et al. (2016) in Table S9, which reveals an increase of 0.78 ± 1.12 % yr<sup>-1</sup> for the MMA, but  
624 decreases of 1.82 ± 0.84 % yr<sup>-1</sup> for the GMA and of 0.10 ± 1.67 % yr<sup>-1</sup> for the MCMA, all during 2005-  
625 2014. To date, long-term trends in VOCs have only been reported only the MCMA with an average  
626 decrease of ca. 2.4 ppb yr<sup>-1</sup> since 2002, mostly in propane, ethanol and acetone (Garzón et al., 2016),  
627 while there are no studies of long-term trends in VOCs within the MMA and the GMA.

628  
629 **It has been shown that O<sub>3</sub> and O<sub>x</sub> decreases within the MCMA have been driven by reductions in NO<sub>x</sub>**  
630 **and VOCs emissions, and that the implemented strategies described in Sect. 4.1 have proved to be**  
631 **effective in controlling primary emissions (ProAire-MCMA, 2011; Jaimes-Palomera et al., 2016).** By  
632 contrast, growing industrial emissions within the MMA must be subject to stringent controls to abate O<sub>3</sub>  
633 levels. In the GMA, where the industrial activity is lower that at the MCMA and MMA (Kanda et al., 2016),  
634 the policies introduced at national scale for controlling on-road sources emissions have resulted in the  
635 decrease of NO<sub>x</sub> emissions and in the stabilisation of O<sub>3</sub> levels. The results presented here demonstrate  
636 the merits of the assessment and analysis of long-term O<sub>3</sub> levels, which can be used by environmental  
637 authorities to revise and to redesign programs and policies to improve air quality. Continuing with ground-  
638 based O<sub>3</sub> and NO<sub>x</sub> monitoring is strongly recommended to better understand the response further  
639 changes in local and regional O<sub>3</sub> levels to changes in primary emissions. Monitoring of VOCs at the GMA  
640 and MMA is also recommended to as the VOCs emissions data reported in the NAEI possess significant  
641 uncertainties. **Finally, according to the results presented here, we recommend preferentially reducing**  
642 **VOCs emissions, which may limit O<sub>3</sub> production in response to a decrease in the VOCs/NO<sub>x</sub> ratio.**  
643 **However, simultaneously reducing NO<sub>x</sub> will have added health benefits of less NO<sub>2</sub>.**

## 645 **5. Conclusions**

646 Diurnal and annual cycles, and long-term trends in  $O_3$  and  $O_x$  within the MMA, are interpreted as  
647 response to changes in  $NO_x$  and VOCs emissions, photochemistry and meteorology. Continuous high-  
648 frequency and high-precision  $O_3$  and  $NO_x$  data recorded during 1993-2014 at 5 sites within the MMA  
649 and at 29 sites within the MCMA, and during 1996-2014 at 10 sites within the GMA, were used to  
650 calculate long-term trends. Within the MMA, the greatest mixing ratios in  $O_3$  were recorded during E and  
651 SE winds, at sites downwind of significant precursors from industrial sources. By contrast, the lowest  $O_3$   
652 mixing ratios were recorded at SNN, and for all sites were observed for the W and SW sectors, where  
653 air masses travel from central Mexico over 100-300 km of semi-arid region sparsely populated. Maximum  
654 daily 1-h values of  $O_3$  and  $O_x$  increased significantly at GPE, SNN and SNB, owing to increasing  
655 emissions of precursors, while at OBI increasing  $O_3$  and decreasing  $O_x$  trends arise from the non-linear  
656 response to decreasing  $NO_x$  emissions from on-road sources.

657

658 Annual cycles in  $O_3$  at all sites peak in spring and through in winter, with a downward spike during  
659 summer caused by high winds that disperse  $O_3$ , and increase the boundary layer height. Decreases in  
660  $O_3$  precursor emissions during the economic crisis experienced in Mexico between 1994-1996, caused  
661 significant decline trends  $O_3$  annual variations from 1993 to 1997 or 1998, depending on site, followed  
662 by significant increases derived from the recovery of the economy. The dominant role of industrial  
663 sources on  $O_3$  precursor levels within the MMA was evident at the industrial site SNN during the 1994-  
664 1996 economic crisis.

665

666 At all metropolitan areas studied,  $O_3$  and  $O_x$  levels showed no significant differences between weekdays  
667 and weekend, although an earlier occurrence of the  $O_3$  peak at the GMA was detected, ascribed to larger  
668 VOCs/ $NO_x$  emission ratio. The lack of the weekend effect was attributed to weekday  $O_3$  production being  
669 limited by VOCs, whereas increases in the VOC/ $NO_x$  ratio during weekends in response to reduced  
670 emissions from mobile sources resulted in similar  $O_3$  mixing ratios that during weekdays. Larger  $AV_{0.5}$   
671 during weekdays and weekends were seen at MCMA than at GMA and MMA related to the relative  
672 emissions of the  $O_3$  precursors.

673

674 Significant seasonal trends in  $O_3$  and  $O_x$  during spring were observed at all sites, apart from STA,  
675 whereas industrial sites exhibited significant increases for  $O_x$  in all seasons. The largest increases in  $O_3$   
676 and  $O_x$  were observed during the occurrence of NE-E-SE air masses. The only significant decrease in  
677  $O_x$  at STA was related to the NW wind occurrence during winter.  $NO_x$  mixing ratios increased significantly  
678 at all sites, except at OBI, due to the dominant role of industrial sources on  $NO_x$  levels. The overall  
679 significant increasing trend of  $0.22 \text{ ppb } O_3 \text{ yr}^{-1}$  within the MMA contrasts within a significant decreasing  
680 trend of  $1.15 \text{ ppb } O_3 \text{ yr}^{-1}$  within the MCMA during 1993-2014, whereas a non-significant trend is evident  
681 within the GMA during 1996-2014. At the MCMA and GMA, the overall  $O_x$  trends reflect the trends in  $O_3$

682 precursors. According to the long-term trends in O<sub>3</sub> for the MMA, the number of exceedances of the air  
683 quality standards will very likely increase as result of increasing precursor emissions. The moderate  
684 mitigation of O<sub>3</sub> levels within the MCMA, derived from measures implemented to control emissions from  
685 on-road, industrial and area sources, emphasises the need for more stringent control of emissions mostly  
686 from industrial sources within the MMA in order to improve air quality. Finally, comparison between  
687 emission inventories estimates of NO<sub>x</sub> and VOCs with ground-based measurements, indicate that  
688 significant reductions in uncertainties are required to better inform air quality policies.

689

## 690 **6. Acknowledgments**

691 This research was supported by Tecnológico de Monterrey through the Research Group for Energy and  
692 Climate Change (Grant 0824A0104 and 002EICIR01). Grateful acknowledgements are made to the  
693 Secretariat for Sustainable Development of the Nuevo Leon State, the Secretariat for the Environment  
694 of Mexico City and the Secretariat for the Environment and Territorial Development of the Jalisco State  
695 for the public domain records. We gratefully thank the NOAA Air Resources Laboratory (ARL) for access  
696 to the HYSPLIT model and READY website (<http://www.ready.noaa.gov>), and Dr. Sigfrido Iglesias for  
697 providing the imputed O<sub>3</sub> and NO<sub>x</sub> data for the MMA time-series. We are also grateful to Professor Paul  
698 Monks and Professor Richard Derwent for encouraging comments on an earlier version of the  
699 manuscript.

700

## 701 **7. References**

702 Akimoto, H., Mori, Y., Sasaki, K., Nakanishi, H., Ohizumi, T., and Itano, Y.: Analysis of monitoring data  
703 of ground-level ozone in Japan for long-term trend during 1990-2010: Causes of temporal and spatial  
704 variation, *Atmos. Environ.*, 102, 302-310, doi:10.1016/j.atmosenv.2014.12.001, 2015.

705 Arriaga-Colina, J. L., West, J. J., Sosa, G., Escalona, S. S., Ordunez, R. M., and Cervantes, A. D. M.  
706 Measurements of VOCs in Mexico City (1992–2001) and evaluation of VOCs and CO in the emissions  
707 inventory, *Atmos. Environ.*, 38, 2523-2533, doi:10.1016/j.atmosenv.2004.01.033, 2004.

708 Atkinson, R.: Atmospheric chemistry of VOCs and NO<sub>x</sub>. *Atmos. Environ.*, 34, 2063-2101,  
709 doi:10.1016/S1352-2310(99)00460-4, 2000.

710 Benítez-García, S. E., Kanda, I., Wakamatsu, S., Okazaki, Y., and Kawano, M.: Analysis of criteria air  
711 pollutant trends in three Mexican metropolitan areas, *Atmosphere*, 5, 806-829,  
712 doi:10.3390/atmos5040806, 2014.

713 Boersma, K. F., Jacob, D. J., Bucsela, E. J., Perring, A. E., Dirksen, R., van der A, R. J., Yantosca, R.  
714 M., Park, R. J., Wenig, M. O., Bertram, T. H., and Cohen, R. C.: Validation of OMI tropospheric NO<sub>2</sub>  
715 observations during INTEX-B and application to constrain NO<sub>x</sub> emissions over the eastern United States  
716 and Mexico, *Atmos. Environ.*, 42, 4480-4497. doi:10.1016/j.atmosenv.2008.02.004, 2008.

717 Butler, T. M., Stock, Z. S., Russo, M. R., Denier Van Der Gon, H. A. C., and Lawrence, M. G.: Megacity  
718 ozone air quality under four alternative future scenarios, *Atmos. Chem. Phys.*, 12, 4413-4428,  
719 doi:10.5194/acp-12-4413-2012, 2012

720 Camalier, L., Cox, W., and Dolwick, P.: The effects of meteorology on ozone in urban areas and their  
721 use in assessing ozone trends, *Atmos. Environ.*, 41, 7127-7137, doi: 10.1016/j.atmosenv.2007.04.061,  
722 2007.

723 Carrillo-Torres, E. R., Hernández-Paniagua, I. Y., and Mendoza, A.: Use of combined observational-and  
724 model-derived photochemical indicators to assess the O<sub>3</sub>-NO<sub>x</sub>-VOC system sensitivity in urban areas,  
725 *Atmosphere*, 8, 22, doi:10.3390/atmos8020022, 2017.

726 Carslaw, D. C., and Ropkins, K.: openair - An R package for air quality data analysis, *Environ. Model.*  
727 *Soft.*, 27-28, 52-61, doi:10.1016/j.envsoft.2011.09.008, 2012.

728 Carslaw, D. C.: The openair manual - open-source tools for analysing air pollution data, Manual for  
729 version 1.1-4, King's College London, 2015.

730 Castellanos, P. and Boersma, K. F.: Reductions in nitrogen oxides over Europe driven by environmental  
731 policy and economic recession, *Sci. Rep.*, 2, doi:10.1038/srep00265, 2012.

732 Clapp, L. J., and Jenkin, M. E.: Analysis of the relationship between ambient levels of O<sub>3</sub>, NO<sub>2</sub> and NO  
733 as a function of NO<sub>x</sub> in the UK. *Atmospheric Environment*, 35, 6391-6405, doi: 10.1016/S1352-  
734 2310(01)00378-8, 2001.

735 Cleveland, R. B., Cleveland, W. S., McRae, J., and Terpenning, I.: STL: A seasonal-trend decomposition  
736 procedure based on Loess, *J. Off. Stats.*, 6, 3-33, 1990.

737 Dentener, F., Stevenson, D., Cofala, J., Mechler, R., Amann, M., Bergamaschi, P., Raes, F., and  
738 Derwent, R.: The impact of air pollutant and methane emission controls on tropospheric ozone and  
739 radiative forcing: CTM calculations for the period 1990-2030, *Atmos. Chem. Phys.*, 5, 1731-1755,  
740 doi:10.5194/acp-5-1731-2005, 2005.

741 Duncan, B. N., Lamsal, L. N., Thompson, A. M., Yoshida, Y., Lu, Z., Streets, D. G., Hurwitz, M. M., and  
742 Pickering, K. E.: A space-based, high-resolution view of notable changes in urban NO<sub>x</sub> pollution around  
743 the world (2005–2014), *J. Geophys. Res.*, 121, 976–996, doi:10.1002/2015JD024121, 2016.

744 Durbin, J., and Koopman, S. J.: *Time Series Analysis by State Space Methods*, Oxford University Press,  
745 Oxford UK, 2nd Edition, 2012.

746 EPA (Environmental Protection Agency US): *Compilation of Air Pollution Emission Factors (AP-42),*  
747 *Volume I: Stationary Point and Area Sources*, available at: [https://www.epa.gov/air-emissions-factors-](https://www.epa.gov/air-emissions-factors-and-quantification/ap-42-compilation-air-emission-factors)  
748 [and-quantification/ap-42-compilation-air-emission-factors](https://www.epa.gov/air-emissions-factors-and-quantification/ap-42-compilation-air-emission-factors), last access: 14 Jan 2017, 1995.

749 EPA (Environmental Protection Agency US): *User's Guide to MOBILE6.1 and MOBILE6.2: Mobile*  
750 *Source Emission Factor Model*, available at: [https://www3.epa.gov/otaq/models/mobile6/](https://www3.epa.gov/otaq/models/mobile6/420r03010.pdf)  
751 [420r03010.pdf](https://www3.epa.gov/otaq/models/mobile6/420r03010.pdf), last access: 16 Jan 2017, 2003.

752 EPA (Environmental Protection Agency US): *Air quality trends*, available at: [https://www.epa.gov/air-](https://www.epa.gov/air-trends)  
753 [trends](https://www.epa.gov/air-trends), last access: 15 Jan 2017, 2009.

754 Garzón, J. P., Huertas, J. I., Magaña, M., Huertas, M. E., Cárdenas, B., Watanabe, T., Maeda, T.,  
755 Wakamatsu, S., and Blanco, S.: Volatile organic compounds in the atmosphere of Mexico City, *Atmos.*  
756 *Environ.*, 119, 415-429, doi:10.1016/j.atmosenv.2015.08.014, 2015.

757 Guicherit, R., and Roemer, M.: Tropospheric ozone trends, *Chemosphere*, 2, 167-183,  
758 doi:10.1016/S1465-9972(00)00008-8, 2000.

759 Hernández-Paniagua, I. Y., Lowry, D., Clemitshaw, K. C., Fisher, R. E., France, J. L., Lanoisellé, M.,  
760 Ramonet, M., and Nisbet, E. G.: Diurnal, seasonal, and annual trends in atmospheric CO<sub>2</sub> at southwest  
761 London during 2000-2012: Wind sector analysis and comparison with Mace Head, Ireland, *Atmos.*  
762 *Environ.*, 105, 138-147, doi: 10.1016/j.atmosenv.2015.01.02, 2015.

763 INE (Instituto Nacional de Ecología): *Cuarto almanaque de datos y tendencias de la calidad del aire en*  
764 *20 ciudades Mexicanas 2000-2009*, INE-SEMARNAT, México, D.F., 405 pp., 2011.

765 INEGI (National Institute of Statistics and Geography): *XIII Censo General de Población y Vivienda 2010*,  
766 México, available at: <http://www.censo2010.org.mx/>, last Access: 22 May 2016, 2010.

767 INEGI (National Institute of Statistics and Geography): México en Cifras, México, available at:  
768 <http://www3.inegi.org.mx/sistemas/mexicocifras/default.aspx?e=19>, last access: 22 May 2016, 2015.

769 INEGI (National Institute of Statistics and Geography): Producto Interno Bruto (GDP)–Trimestral 2016,  
770 available at: <http://www.inegi.org.mx/est/contenidos/proyectos/cn/pibt/>, last access: 11 Jan 2017, 2016.

771 IPCC: Climate Change 2013: The Physical Science Basis. Contribution of Working Group I to the Fifth  
772 Assessment Report of the Intergovernmental Panel on Climate Change, 2013. [Stocker, T.F., D. Qin, G.-  
773 K. Plattner, M. Tignor, S.K. Allen, J. Boschung, A. Nauels, Y. Xia, V. Bex and P.M. Midgley (eds.)].  
774 Cambridge University Press, Cambridge, United Kingdom and New York, NY, USA, 1535 pp., 2013.

775 Jaimes, P. M., Bravo, A. H., Sosa, E. R., Cureño, G. I., Retama, H. A., Granados, G. G., and Becerra,  
776 A. E.: Surface ozone concentration trends in Mexico City Metropolitan Area, in: Proceedings of the Air  
777 and Waste Management Association's Annual Conference and Exhibition AWMA, San Antonio, Texas,  
778 19-22 June 2012, 3, 2273-2284, 2012.

779 Jaimes-Palomera, M., Retama, A., Elias-Castro, G., Neria-Hernández, A., Rivera-Hernández, O., and  
780 Velasco, E.: Non-methane hydrocarbons in the atmosphere of Mexico City: Results of the 2012 ozone-  
781 season campaign, *Atmos. Environ.*, 132, 258-275, doi:10.1016/j.atmosenv.2016.02.047, 2016.

782 Jenkin, M. E., and Clemitshaw, K. C.: Ozone and other secondary photochemical pollutants: chemical  
783 processes governing their formation in the planetary boundary layer, *Atmos. Environ.*, 34(16), 2499-  
784 2527, doi:10.1016/S1352-2310(99)00478-1, 2000.

785 Kanda, I., Basaldud, R., Magaña, M., Retama, A., Kubo, R., and Wakamatsu, S.: Comparison of Ozone  
786 Production Regimes between Two Mexican Cities: Guadalajara and Mexico City, *Atmosphere*, 7, 91,  
787 doi:10.3390/atmos7070091, 2016.

788 Lee, Y. C., Shindell, D. T., Faluvegi, G., Wenig, M., Lam, Y. F., Ning, Z., Hao, S., and Lai, C. S.: Increase  
789 of ozone concentrations, its temperature sensitivity and the precursor factor in South China, *Tellus B*.  
790 *Chem. Phys. Meteorol.*, 66, doi:10.3402/tellusb.v66.23455, 2014.

791 Lefohn, A. S., Shadwick, D., and Oltmans, S. J.: Characterizing changes in surface ozone levels in  
792 metropolitan and rural areas in the United States for 1980-2008 and 1994-2008, *Atmos. Environ.*, 44,  
793 5199–5210, doi: 10.1016/j.atmosenv.2010.08.049, 2010.

794 Lei, W., de Foy, B., Zavala, M., Volkamer, R., and Molina, L. T.: Characterizing ozone production in the  
795 Mexico City Metropolitan Area: a case study using a chemical transport model, *Atmos. Chem. Phys.*, 7,  
796 1347-1366, doi:10.5194/acp-7-1347-2007, 2007.

797 Lelieveld, J., Evans, J. S., Fnais, M., Giannadaki, D., and Pozzer, A.: The contribution of outdoor air  
798 pollution sources to premature mortality on a global scale, *Nature Letts.*, 15371,  
799 doi:10.1038/nature15371, 2015.

800 Menchaca-Torre, H. L., Mercado-Hernández, R., and Mendoza-Domínguez, A.: Diurnal and seasonal  
801 variation of volatile organic compounds in the atmosphere of Monterrey, Mexico, *Atmos. Poll. Res.*, 6,  
802 1073-1081, doi:10.1016/j.apr.2015.06.004, 2015.

803 Molina, M. J., and Molina, L. T.: Megacities and atmospheric pollution, *J. Air Waste Manage.*, 54, 644-  
804 680, doi:10.1080/10473289.2004.10470936, 2004.

805 Monks, P. S.: A review of the observations and origins of the spring ozone maximum, *Atmos. Environ.*,  
806 34, 3545-3561, doi:10.1016/S1352-2310(00)00129-1, 2000.

807 Monks, P. S., Archibald, A. T., Colette, A., Cooper, O., Coyle, M., Derwent, R., Fowler, D., Granier, C.,  
808 Law, K. S., Mills, G. E., Stevenson, D. S., Tarasova, O., Thouret, V., von Schneidmesser, E.,  
809 Sommariva, R., Wild, O., and Williams, M. L.: Tropospheric ozone and its precursors from the urban to  
810 the global scale from air quality to short-lived climate forcer, *Atmos. Chem. Phys.*, 15, 8889-8973,  
811 doi:10.5194/acp-15-8889-2015, 2015.



812 Parrish, D. D., Millet, D. B., and Goldstein, A. H.: Increasing ozone in marine boundary layer inflow at  
813 the west coasts of North America and Europe, *Atmos. Chem. Phys.*, 9, 1303-1323, doi:10.5194/acp-9-  
814 1303-2009, 2009.

815 Parrish, D. D., Singh, H. B., Molina, L., and Madronich, S.: Air quality progress in North American  
816 megacities: A review, *Atmos. Environ.*, 45, 7015-7025, doi:10.1016/j.atmosenv.2011.09.039, 2011.

817 PICCA (Programa integral contra la contaminación atmosférica de la zona metropolitana de la Ciudad  
818 de México), Mexico City Local Government, available at: [http://centro.paot.org.mx/documentos/  
819 varios/prog\\_inte\\_atmosferica.pdf](http://centro.paot.org.mx/documentos/varios/prog_inte_atmosferica.pdf), last Access: 28 April 2017, 1990

820 ProAire-MMA (Programa de Gestión para Mejorar la Calidad del Aire del Área Metropolitana de  
821 Monterrey 2008-2012), SEMARNAT, Gobierno del estado de Nuevo León, available at:  
822 [http://www.semarnat.gob.mx/archivosanteriores/temas/gestionambiental/calidaddelaire/  
823 Documents/Calidad%20del%20aire/Proaires/ProAires\\_Vigentes/6\\_ProAire%20AMM%202008-  
824 2012.pdf](http://www.semarnat.gob.mx/archivosanteriores/temas/gestionambiental/calidaddelaire/Documents/Calidad%20del%20aire/Proaires/ProAires_Vigentes/6_ProAire%20AMM%202008-2012.pdf), last access: 22 May 2016, 2008.

825 ProAire-MCMA (Programa para Mejorar la Calidad del Aire de la Zona Metropolitana del Valle de México  
826 2002-2010), Mexico City Local Government-State of Mexico Government, available at:  
827 [http://www.gob.mx/cms/uploads/attachment/file/69312/11\\_ProAire\\_ZMVM\\_2002-2010.pdf](http://www.gob.mx/cms/uploads/attachment/file/69312/11_ProAire_ZMVM_2002-2010.pdf), last access:  
828 28 April, 2017, 2001.

829 ProAire-MCMA (Programa para Mejorar la Calidad del Aire de la Zona Metropolitana del Valle de México  
830 2002-2010), Mexico City Local Government-State of Mexico Government, available at:  
831 <http://www.aire.cdmx.gob.mx/descargas/publicaciones/flippingbook/proaire2011-2020/#p=1>, last  
832 access: 28 April 2017, 2011

833 Pugliese, S. C., Murphy, J. G., Geddes, J. A., and Wang, J. M.: The impacts of precursor reduction and  
834 meteorology on ground-level ozone in the Greater Toronto Area, *Atmos. Chem. Phys.*, 14, 8197-8207,  
835 doi:10.5194/acp-14-8197-2014, 2014.

836 Pusede, S. E., and Cohen, R. C. On the observed response of ozone to NO<sub>x</sub> and VOC reactivity  
837 reductions in San Joaquin Valley California 1995–present, *Atmos. Chem. Phys.*, 12, 8323-8339,  
838 doi:10.5194/acp-12-8323-2012, 2012.

839 Pusede, S. E., Steiner, A. L., and Cohen, R.C.: Temperature and recent trends in the chemistry of  
840 continental surface ozone, *Chem. Rev.*, 115, 3898-3918, doi: 10.1021/cr5006815, 2015.

841 R Core Team: R: a Language and Environment for Statistical Computing, R Foundation for Statistical  
842 Computing, Vienna, Austria, ISBN 3-900051-07-0, 2013, available at: [www.R-project.org](http://www.R-project.org), last access:  
843 23 May 2016, 2013.

844 Radian (International): Mexico Emissions Inventory Program Manuals (Vol. II-VI), available at:  
845 [https://www3.epa.gov/ttnecat1/cica/other3\\_s.html](https://www3.epa.gov/ttnecat1/cica/other3_s.html), last access: 15 Jan 2017, 2000.

846 Reinsel, G. C.: Elements of Multivariate Time Series Analysis. Springer-Verlag, New York, USA, 2nd  
847 Edition, 1997.

848 Revell, L. E., Tummon, F., Stenke, A., Sukhodolov, T., Coulon, A., Rozanov, E., Garny, H., Grewe, V.  
849 and Peter, T.: Drivers of the tropospheric ozone budget throughout the 21st century under the medium-  
850 high climate scenario RCP 6.0, *Atmos. Chem. Phys.*, 15, 5887-5902, doi:10.5194/acp-15-5887-2015,  
851 2015.

852 Rodríguez, S., Huerta, G., and Reyes, H.: A study of trends for Mexico City ozone extremes: 2001-2014,  
853 *Atmosfera*, 29, 107-120, doi:10.20937/ATM.2016.29.02.01, 2016.

854 Russell, A. R., Valin, L. C., and Cohen, R. C.: Trends in OMI NO<sub>2</sub> observations over the United States:  
855 effects of emission control technology and the economic recession, *Atmos. Chem. Phys.*, 12, 12197-  
856 12209, doi:10.5194/acp-12-12197-2012, 2012.

857 Salmi, T., Määttä, A., Anttila, P., Ruoho-Airola, T. and Amnell, T.: Detecting trends of annual values of  
858 atmospheric pollutants by the Mann-Kendall test and Sen's slope estimates – the Excel template  
859 application MAKESENS, Publications on Air Quality Report code FMI-AQ-31, Helsinki, Finland, 31, 1-  
860 35, 2002.

861 Schultz, M., and Rast, S.: REanalysis of the TROpospheric chemical composition over the past 40 years,  
862 Emission Data Sets and Methodologies for Estimating Emissions, Work Package 1, Deliverable D1-6,  
863 available at: [http://retro-archive.iek.fz-juelich.de/data/documents/reports/D1-6\\_final.pdf](http://retro-archive.iek.fz-juelich.de/data/documents/reports/D1-6_final.pdf), last access: 14  
864 Jul 2016, 2007.

865 SDS (Secretaria de Desarrollo Sustentable), Inventario de emisiones del Área Metropolitana de  
866 Monterrey 2013, personal communication, Monterrey, N.L. México, 4 Sep 2015.

867 SDS (Secretaria de Desarrollo Sustentable): Sistema Integral de Monitoreo Ambiental, available at:  
868 <http://aire.nl.gob.mx/>, last access: 21 May 2016, 2016.

869 SEDEMA (Secretaria del Medio Ambiente): INVENTARIO de Emisiones a la Atmosfera en la ZMVM  
870 1996, available at: <http://www.sedema.df.gob.mx/flippingbook/inventario-emisiones-1996/#p=1>, last  
871 access: 20 May 2016, 1999.

872 SEDEMA (Secretaria del Medio Ambiente): Inventario de Emisiones Zona Metropolitana del Valle de  
873 Mexico 1998, available at: [http://www.sedema.df.gob.mx/flippingbook/inventario-emisiones-  
874 zmvm1998/#p=75](http://www.sedema.df.gob.mx/flippingbook/inventario-emisiones-zmvm1998/#p=75), last access: 20 May 2016, 2001.

875 SEDEMA (Secretaria del Medio Ambiente): Inventario de emisiones a la Atmosfera Zona Metropolitana  
876 del Valle de Mexico 2000, available at: [http://www.sedema.df.gob.mx/ flippingbook/inventario-  
877 emisiones-zmvm2000/](http://www.sedema.df.gob.mx/flippingbook/inventario-emisiones-zmvm2000/), last access: 20 May 2016, 2003.

878 SEDEMA (Secretaria del Medio Ambiente): Inventario de emisiones de la Zona Metropolitana del Valle  
879 de Mexico 2002, available at: [http://www.sedema.df.gob.mx/flippingbook/inventario-emisiones-zmvm-  
880 criterio2004/#p=1](http://www.sedema.df.gob.mx/flippingbook/inventario-emisiones-zmvm-criterio2004/#p=1), last access: 20 May 2016, 2004.

881 SEDEMA (Secretaria del Medio Ambiente): Inventario de Emisiones Zona Metropolitana del Valle de  
882 Mexico 2004, available at: [http://www.sedema.df.gob.mx/flippingbook/inventario-emisiones-zmvm-  
883 criterio2004/#p=1](http://www.sedema.df.gob.mx/flippingbook/inventario-emisiones-zmvm-criterio2004/#p=1), last access: 20 May 2016, 2006.

884 SEDEMA (Secretaria del Medio Ambiente): Inventario de Emisiones de Contaminantes Criterio 2006,  
885 available at: <http://www.sedema.df.gob.mx/flippingbook/inventario-emisiones-zmvm-criterio2006/#p=1>,  
886 last access: 20 May 2016, 2008.

887 SEDEMA (Secretaria del Medio Ambiente): Inventario de emisiones de contaminantes criterio de la  
888 ZMVM 2008, available at: [http://www.sedema.df.gob.mx/flippingbook/inventario-emisiones-zmvm-  
889 criterio2008/#p=1](http://www.sedema.df.gob.mx/flippingbook/inventario-emisiones-zmvm-criterio2008/#p=1), last access: 20 May 2016, 2010.

890 SEDEMA (Secretaria del Medio Ambiente): Inventario de emisiones de la Zona Metroplitiana del Valle  
891 de Mexico contaminantes criterio 2010, available at:  
892 <http://www.sedema.df.gob.mx/flippingbook/inventario-em1isiones-zmvm-criterio-2010/#p=6>, last  
893 access: 20 May 2016, 2012.

894 SEDEMA (Secretaria del Medio Ambiente): Inventario de Emisiones Contaminantes y de efecto  
895 invernadero, available at: <http://www.sedema.df.gob.mx/flippingbook/inventario-emisioneszmvm2012/>,  
896 last access: 20 May 2016, 2014.

897 SEDEMA (Secretaria del Medio Ambiente de la Ciudad de Mexico): Sistema de Monitoreo Atmosférico,  
898 available at: <http://www.aire.df.gob.mx/default.php>, last access: 21 May 2016, 2016a.

899 SEDEMA (Secretaria del Medio Ambiente de la Ciudad de Mexico): Inventario de Emisiones de la CDMX  
900 2014 Contaminantes Criterio Tóxicos y de Efecto Invernadero, available at:  
901 <http://www.aire.cdmx.gob.mx/descargas/publicaciones/flippingbook/inventario-emisiones-cdmx2014-2/>,  
902 last Access: 10 Jan 2017, 2016b.

903 SEMARNAT (Secretaria del Medio Ambiente y Recursos Naturales): NOM-041 (NORMA OFICIAL  
904 MEXICANA, QUE ESTABLECE LOS LIMITES MAXIMOS PERMISIBLES DE EMISION DE GASES  
905 CONTAMINANTES PROVENIENTES DEL ESCAPE DE LOS VEHICULOS AUTOMOTORES EN  
906 CIRCULACION QUE USAN GASOLINA COMO COMBUSTIBLE), Diario Oficial de la Federación, 1993.

907 SEMARNAT (Secretaria del Medio Ambiente y Recursos Naturales): NOM-042 (NORMA OFICIAL  
908 MEXICANA QUE ESTABLECE LOS LIMITES MAXIMOS PERMISIBLES DE EMISION DE  
909 HIDROCARBUROS TOTALES O NO METANO, MONOXIDO DE CARBONO, OXIDOS DE  
910 NITROGENO Y PARTICULAS PROVENIENTES DEL ESCAPE DE LOS VEHICULOS  
911 AUTOMOTORES NUEVOS CUYO PESO BRUTO VEHICULAR NO EXCEDA LOS 3,857  
912 KILOGRAMOS, QUE USAN GASOLINA, GAS LICUADO DE PETROLEO, GAS NATURAL Y DIESEL,  
913 ASI COMO DE LAS EMISIONES DE HIDROCARBUROS EVAPORATIVOS PROVENIENTES DEL  
914 SISTEMA DE COMBUSTIBLE DE DICHS VEHICULOS), Diario Oficial de la Federación, 1993.

915 SEMARNAT (Secretaria del Medio Ambiente y Recursos Naturales): Inventario Nacional de Emisiones  
916 1999, México, D.F., available at: <http://www.inecc.gob.mx/dica/548-calair-inem-1999>, last access: 20  
917 May 2016, 2006.

918 SEMARNAT (Secretaria del Medio Ambiente y Recursos Naturales): Inventario Nacional de Emisiones  
919 2005, México, D.F., available at: <http://sinea.semarnat.gob.mx/sinae.php?process=UkVQT1JURUFET1I=&categ=1>, last access: 22 May 2016, 2011.

921 SEMARNAT (Secretaria del Medio Ambiente y Recursos Naturales): Inventario Nacional de Emisiones  
922 2008, México, D.F., available at: <http://sinea.semarnat.gob.mx/sinae.php?process=UkVQT1JURUFET1I=&categ=14>, last access: 22 May 2016, 2014.

924 SEMARNAT (Secretaria del Medio Ambiente y Recursos Naturales): Informe Nacional de calidad del  
925 aire 2014, México, D.F., available at: [http://inecc.gob.mx/descargas/calair/2015\\_Informe\\_nacional\\_calidad\\_aire\\_2014\\_Final.pdf](http://inecc.gob.mx/descargas/calair/2015_Informe_nacional_calidad_aire_2014_Final.pdf), last access: 15 Dec 2016, 2015.

927 SENER (Secretaria de Energia): Estadísticas Energéticas Nacionales, México, available at:  
928 <http://sie.energia.gob.mx/bdiController.do?action=temas>, last access: 4 November 2015, 2015.

929 Sicard, P., Serra, R., and Rossello, P.: Spatiotemporal trends in ground-level ozone concentrations and  
930 metrics in France over the time period 1999-2012, *Environ. Res.*, 149, 122-144,  
931 doi:10.1016/j.envres.2016.05.014, 2016

932 Sierra, A., Vanoye, A. Y., and Mendoza, A.: Ozone sensitivity to its precursor emissions in northeastern  
933 Mexico for a summer air pollution episode, *J. Air Waste Manage.*, 63, 1221-1233,  
934 doi:10.1080/10962247.2013.813875, 2013.

935 Simon, H., Reff, A., Wells, B., Xing, J., and Frank, N.: Ozone trends across the United States over a  
936 period of decreasing NO<sub>x</sub> and VOC emissions, *Environ. Sci. Tech.*, 49, 186-195. doi:10.1021/es504514z,  
937 2015.

938 SMN (Servicio Meteorológico Nacional), available at: <http://smn.cna.gob.mx/es/>, last access: 21 May  
939 2016.

940 Staehelin, J., and Schmid, W.: Trend analysis of tropospheric ozone concentrations utilizing the 20-year  
941 data set of ozone balloon soundings over Payerne (Switzerland), *Atmos. Environ.*, 25, 1739-1749,  
942 doi:10.1016/0960-1686(91)90258-9, 1991.

943 Stein, A. F., Draxler, R. R., Rolph, G. D., Stunder, B. J. B., Cohen, M. D., and Ngan, F.: NOAA'S HYSPLIT  
944 atmospheric transport and dispersion modelling system. *Am. Meteorol. Soc.*, 96, 2059-2077,  
945 doi:10.1175/BAMS-D-14-00110.1, 2015.

946 Stephens, S., Madronich, S., Wu, F., Olson, J. B., Ramos, R., Retama, A., and Muñoz, R.: Weekly  
947 patterns of México City's surface concentrations of CO, NO<sub>x</sub>, PM<sub>10</sub> and O<sub>3</sub> during 1986-2007, *Atmos.*  
948 *Chem. Phys.*, 8, 5313-5325, doi:10.5194/acp-8-5313-2008, 2008.

949 Stevenson, D. S., Dentener, F. J., Schultz, M. G., Ellingsen, K., van Noije, T. P. C., Wild, O., Zeng, G.,  
950 Amann, M., Atherton, C. S., Bell, N., Bergmann, D. J., Bey, I., Butler, T., Cofala, J., Collins, W. J.,  
951 Derwent, R. G., Doherty, R. M., Drevet, J., Eskes, H. J., Fiore, A. M., Gauss, M., Hauglustaine, D. A.,  
952 Horowitz, L. W., Isaksen, I. S. A., Krol, M. C., Lamarque, J.-., Lawrence, M. G., Montanaro, V., Müller,  
953 J.-., Pitari, G., Prather, M. J., Pyle, J. A., Rast, S., Rodriguez, J. M., Sanderson, M. G., Savage, N. H.,  
954 Shindell, D. T., Strahan, S. E., Sudo, K., and Szopa, S.: Multimodel ensemble simulations of present-  
955 day and near-future tropospheric ozone. *J. Geophys. Res.*, D08301, doi: 10.1029/2005JD006338, 2006.

956 Strode, S. A., Rodriguez, J. M., Logan, J. A., Cooper, O. R., Witte, J. C., Lamsal, L. N., Damon, M., Van  
957 Aartsen, B., Steenrod, S. D., and Strahan, S. E.: Trends and variability in surface ozone over the United  
958 States, *J. Geophys. Res.*, 120, 9020-9042, doi:10.1002/2014JD022784, 2015.

959 Tiwari, A. K., Suresh, K. G., Arouri, M., and Teulon, F.: Causality between consumer price and producer  
960 price: Evidence from Mexico, *Econ. Model.*, 36, 432-440, doi:10.1016/j.econmod.2013.09.050, 2014.

961 Torres-Jardon, R., García-Reynoso, J. A., Jazcilevich, A., Ruiz-Suárez, L. G., and Keener, T. C.:  
962 Assessment of the ozone-nitrogen oxide-volatile organic compound sensitivity of Mexico City through an  
963 indicator-based approach: measurements and numerical simulations comparison, *J. Air Waste Manag.*  
964 *Assoc.*, 59, 1155-1172, doi:10.3155/1047-3289.59.10.1155, 2009.

965 VanCuren, R.: Transport aloft drives peak ozone in the Mojave Desert, *Atmos. Environ.*, 109, 331-341,  
966 doi: 10.1016/j.atmosenv.2014.09.057, 2015.

967 Vingarzan, R.: A review of surface ozone background levels and trends, *Atmos. Environ.*, 38, 3431-3442,  
968 doi:10.1016/j.atmosenv.2004.03.030, 2004.

969 Velasco, E., Lamb, B., Westberg, H., Allwine, E., Sosa, G., Arriaga-Colina, J. L., Jobson, B. T.,  
970 Alexander, M. L., Prazeller, P., Knighton, W. B., Rogers, T. M., Grutter, M., Herndon, S. C., Kolb, C. E.,  
971 Zavala, M., de Foy, B., Volkamer, R., Molina, L. T., and Molina, M. J.: Distribution, magnitudes,  
972 reactivities, ratios and diurnal patterns of volatile organic compounds in the Valley of Mexico during the  
973 MCMA 2002 & 2003 field campaigns, *Atmos. Chem. Phys.*, 7, 329-353, doi:10.5194/acp-7-329-2007,  
974 2007.

975 Wang, Y., Konopka, P., Liu, Y., Chen, H., Müller, R., Plöger, F., Riese, M., Cai, Z., and Lü, D.:  
976 Tropospheric ozone trend over Beijing from 2002-2010: Ozone-sonde measurements and modeling  
977 analysis, *Atmos. Chem. Phys.*, 12, 8389-8399, doi:10.5194/acp-12-8389-2012, 2012.

978 Wilson, R. C., Fleming, Z. L., Monks, P. S., Clain, G., Henne, S., Konovalov, I. B., Szopa, S., and Menut,  
979 L.: Have primary emission reduction measures reduced ozone across Europe? An analysis of European  
980 rural background ozone trends 1996-2005, *Atmos. Chem. Phys.*, 12, 437-454, doi:10.5194/acp-12-437-  
981 2012, 2012.

982 Wolff, G. T., Kahlbaum, D. F., and Heuss, J. M.: The vanishing ozone weekday/weekend effect, *J. Air  
983 Waste Manage.*, 63, 292-299, doi:10.1080/10962247.2012.749312, 2013.

984 World Health Organization: Ambient (outdoor) air quality and health, 2014 update,  
985 <http://www.who.int/mediacentre/factsheets/fs313/en/>, last access: 21 May 2016.

986 Xing, J., Pleim, J., Mathur, R., Pouliot, G., Hogrefe, C., Gan, C.-M., and Wei, C.: Historical gaseous and  
987 primary aerosol emissions in the United States from 1990 to 2010, *Atmos. Chem. Phys.*, 13, 7531-7549,  
988 doi:10.5194/acp-13-7531-2013, 2013.

989 Xu, X., Lin, W., Wang, T., Yan, P., Tang, J., Meng, Z., and Wang, Y.: Long-term trend of surface ozone  
990 at a regional background station in eastern China 1991-2006: Enhanced variability, *Atmos. Chem. Phys.*,  
991 8, 2595-2607, doi:10.5194/acp-8-2595-2008, 2008.

992 Zellweger, C., Hüglin, C., Klausen, J., Steinbacher, M., Vollmer, M., and Buchmann, B.: Inter-comparison  
993 of four different carbon monoxide measurement techniques and evaluation of the long-term carbon  
994 monoxide time series of Jungfraujoch, *Atmos. Chem. Phys.*, 9, 3491-3503, doi:10.5194/acp-9-3491-  
995 2009, 2009.

996 Zheng, J., Swall, J. L., Cox, W. M., and Davis, J. M. Interannual variation in meteorologically adjusted  
 997 ozone levels in the eastern United States: A comparison of two approaches, *Atmos. Environ.*, 41, 705-  
 998 716, doi:10.1016/j.atmosenv.2006.09.010, 2007.

999

1000

1001

1002 **Table 1.** Air quality limit values stated in Mexican legislation.

Pollutant	Mexican Official Standard	Limit value*
O <sub>3</sub> (ppb)	NOM-020-SSA1-1993	110 (1-h), 80 (8-h) <sup>a,b</sup>
	NOM-020-SSA1-2014	95 (1-h) , 70 (8-h) <sup>a,b</sup>
PM <sub>10</sub> (µg m <sup>-3</sup> )	NOM-025-SSA1-1993	75 (24-h), 40 (1-yr)
	NOM-025-SSA1-2014	50 (24h), 35 (1-yr)
PM <sub>2.5</sub> (µg m <sup>-3</sup> )	NOM-025-SSA1-1993	45 (24-h), 12 (1-yr)
	NOM-025-SSA1-2014	30 (24-h), 10 (1-yr)
CO (ppm)	NOM-02-SSA1-1993	11 (8-h) <sup>b</sup>
NO <sub>2</sub> (ppm)	NOM-023-SSA1 -1993	0.21 (1-h)

1003 \*Average period.

1004 <sup>a</sup>Not to be exceeded more than 4 times in a calendar year.

1005 <sup>b</sup>Running average.

1006

1007

1008 **Table 2.** Site description, location and instrumentation used during 1993 to 2014 within the MMA.

Site	Code	Location	Elevation (m a.s.l.)	Site description
Guadalupe	GPE	25° 40.110' N, 100° 14.907' W	492	Urban background site in the La Pastora park, surrounded by a highly populated area, 450 m from Pablo Rivas Rd.
San Nicolas	SNN	25° 44.727' N, 100° 15.301' W	476	Urban site surrounded by a large number of industries and residential areas, 450 m from Juan Diego Diaz de Beriagna Rd.
Obispado	OBI	25° 40.561' N, 100° 20.314' W	560	Urban site near the city centre of MMA, 250 m from Jose Eleuterio González Rd. and 250 m from Antonio L. Rodríguez Rd.
San Bernabe	SNB	25° 45.415' N, 100° 21.949' W	571	Urban site in a residential area downwind of an industrial area with high traffic volume, 140 m from Aztlan Rd.
Santa Catarina	STA	25° 40.542' N, 100° 27.901' W	679	Urban site downwind of industrial sources, 200 m from Manuel Ordoñez Rd.

1009

1010

1011

1012

1013

1014

1015

1016

1017

1018

1019

1020

1021  
1022

**Table 3.** Results for O<sub>3</sub> and O<sub>x</sub> long-term trends expressed in ppb yr<sup>-1</sup> for 1993-2014 at the 5 sites within the MMA by season.

Site	Period	Ozone (O <sub>3</sub> )			Odd oxygen (O <sub>x</sub> = O <sub>3</sub> + NO <sub>2</sub> )		
		ppb yr <sup>-1</sup>	% yr <sup>-1</sup>	Significance	ppb yr <sup>-1</sup>	% yr <sup>-1</sup>	Significance
GPE	Annual	0.21	0.78	*	0.31	0.80	**
	Spring	0.24	0.73	*	0.32	0.69	*
	Summer	0.30	1.16	*	0.38	1.18	*
	Autumn	0.14	0.53		0.25	0.62	
	Winter	0.12	0.53		0.14	0.33	*
SNN	Annual	0.33	1.40	***	0.45	1.25	*
	Spring	0.39	1.38	*	0.49	1.22	*
	Summer	0.47	2.24	*	0.58	1.87	***
	Autumn	0.41	1.96	*	0.65	1.94	*
	Winter	0.14	0.68		0.23	0.58	+
OBI	Annual	0.30	1.29	*	-0.17	-0.35	
	Spring	0.43	1.56	*	0.02	0.03	*
	Summer	0.26	0.98	*	-0.04	-0.09	
	Autumn	0.29	1.33	+	-0.66	-1.15	
	Winter	0.25	1.46		-0.28	-0.53	
SNB	Annual	0.19	0.65	+	0.61	1.66	**
	Spring	0.37	1.07	+	0.67	1.65	+
	Summer	0.31	1.06	***	0.66	2.17	***
	Autumn	0.19	0.64		0.60	1.61	+
	Winter	0.02	0.07		0.47	1.12	+
STA	Annual	0.01	0.01		-0.15	-0.28	
	Spring	-0.04	-0.11		-0.01	-0.02	
	Summer	0.09	0.28		0.13	0.27	
	Autumn	0.00	0.00		-0.22	-0.41	
	Winter	-0.09	-0.43		-0.63	-1.15	*

1023  
1024  
1025  
1026  
1027  
1028  
1029  
1030  
1031  
1032  
1033

+Level of significance  $p < 0.1$ .  
 \*Level of significance  $p < 0.05$ .  
 \*\*Level of significance  $p < 0.001$ .  
 \*\*\*Level of significance  $p < 0.001$ .

1034  
 1035  
 1036  
 1037  
 1038  
 1039  
 1040  
 1041  
 1042  
 1043  
 1044  
 1045  
 1046  
 1047  
 1048  
 1049  
 1050  
 1051  
 1052  
 1053  
 1054

**Table 4.** Results for O<sub>3</sub> and O<sub>x</sub> long-term trends by season expressed in ppb yr<sup>-1</sup> during 1993-2014 for the MCMA and MMA, and during 1996-2014 for the GMA.

Urban area	Period	Ozone (O <sub>3</sub> )			Odd oxygen (O <sub>3</sub> + NO <sub>2</sub> )		
		ppb yr <sup>-1</sup>	% yr <sup>-1</sup>	Significance	ppb yr <sup>-1</sup>	% yr <sup>-1</sup>	Significance
MCMA	Annual	-1.15	-2.04	***	-1.87	-1.94	***
	Spring	-0.97	-1.53	***	-1.77	-1.71	***
	Summer	-0.97	-1.88	***	-1.44	-1.67	***
	Autumn	-1.12	-2.20	***	-1.89	-2.15	***
	Winter	-1.62	-2.64	***	-2.47	-2.27	***
GMA	Annual	-0.29	-0.81		-1.46	-1.85	+
	Spring	-0.26	-0.57		-1.89	-2.07	*
	Summer	-0.10	-0.32		-1.43	-1.89	*
	Autumn	-0.09	0.33		-1.40	-1.97	*
	Winter	-0.34	-1.01		-1.74	-2.08	***
MMA	Annual	0.22	0.84	**	0.13	0.30	
	Spring	0.32	1.04	**	0.29	0.63	
	Summer	0.27	0.99	***	0.28	0.72	***
	Autumn	0.25	1.03		0.13	0.31	
	Winter	0.10	0.45		0.01	-0.01	

<sup>+</sup>Level of significance  $p < 0.1$ .  
 \*Level of significance  $p < 0.05$ .  
 \*\*Level of significance  $p < 0.001$ .  
 \*\*\*Level of significance  $p < 0.001$ .

1055  
1056

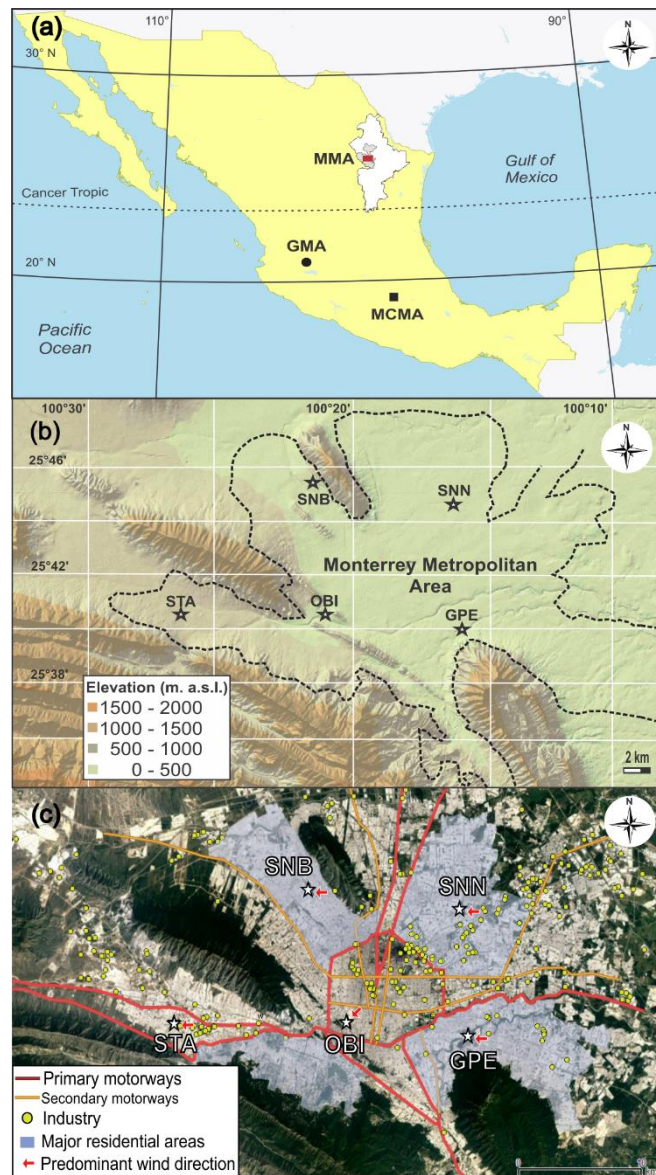
**Table 5.** Results for O<sub>3</sub> daily maxima long-term trends by season in ppb yr<sup>-1</sup> during 1993-2014 at the 5 sites within the MMA.

Site	Period	Ozone (O <sub>3</sub> )		
		ppb yr <sup>-1</sup>	% yr <sup>-1</sup>	Significance
GPE	Annual	0.45	1.02	**
	Spring	0.48	0.94	**
	Summer	0.64	1.50	*
	Autumn	0.35	0.74	
	Winter	0.26	0.63	
SNN	Annual	0.79	2.13	***
	Spring	0.87	2.01	***
	Summer	0.85	2.42	***
	Autumn	0.93	2.73	*
	Winter	0.44	1.29	
OBI	Annual	0.65	1.51	*
	Spring	0.78	1.62	**
	Summer	0.53	1.10	*
	Autumn	0.75	1.77	
	Winter	0.21	0.55	
SNB	Annual	0.40	0.80	***
	Spring	0.85	1.58	***
	Summer	0.67	1.36	***
	Autumn	0.52	1.05	*
	Winter	0.05	0.10	
STA	Annual	0.01	-0.01	
	Spring	-0.05	-0.09	
	Summer	0.22	0.35	
	Autumn	-0.07	-0.12	
	Winter	-0.35	-0.75	+

1057  
1058  
1059  
1060  
1061  
1062

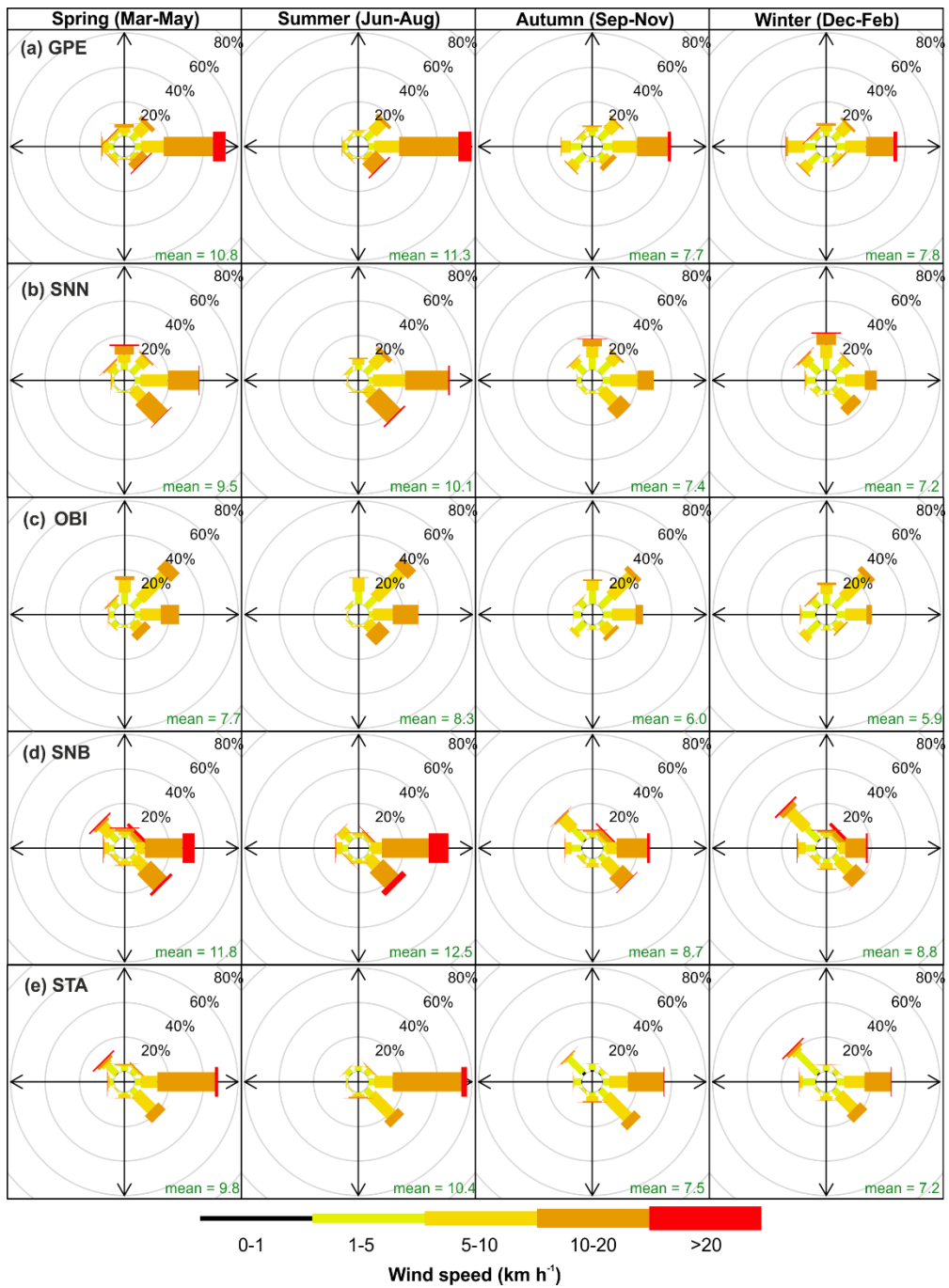
+Level of significance  $p < 0.1$ .  
 \*Level of significance  $p < 0.05$ .  
 \*\*Level of significance  $p < 0.001$ .  
 \*\*\*Level of significance  $p < 0.001$ .





1063  
 1064  
 1065  
 1066  
 1067  
 1068  
 1069  
 1070

**Fig. 1(a).** The MMA, MCMA and GMA in the national context. **(b).** Topography of the MMA and distribution of the 5 monitoring sites over the area. **(c).** The 5 monitoring sites in relation to primary and secondary motorways, industries and major residential areas. The red arrows show the predominant wind direction at each site during 1993 to 2014.



1071  
1072  
1073  
1074

**Fig. 2.** Frequency of counts of measured wind direction occurrence by season and site within the MMA during 1993-2014.

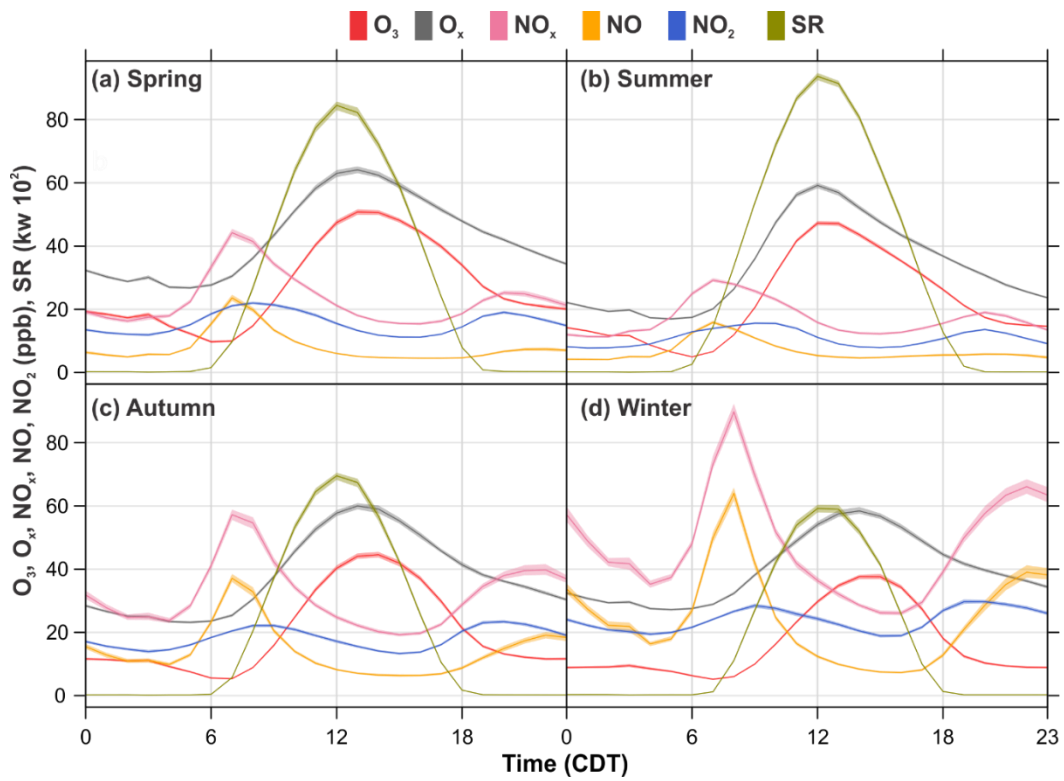


**Fig. 3.** Seasonal average daily profiles for  $O_3$ ,  $O_x$ ,  $NO_x$ ,  $NO$ ,  $NO_2$  and  $SR$  within the MMA during 1993-2014. The shading shows the 95 % confidence intervals of the average.

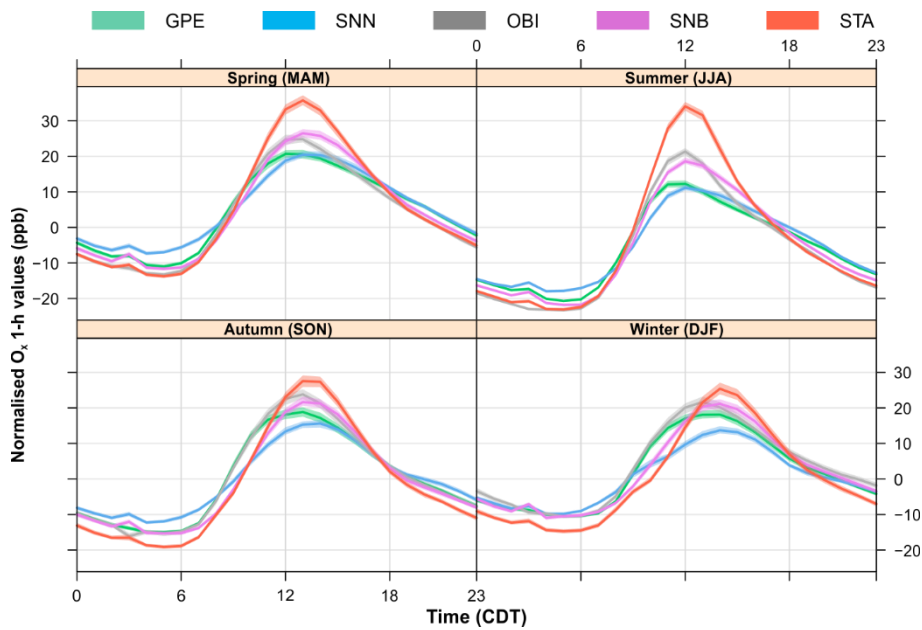
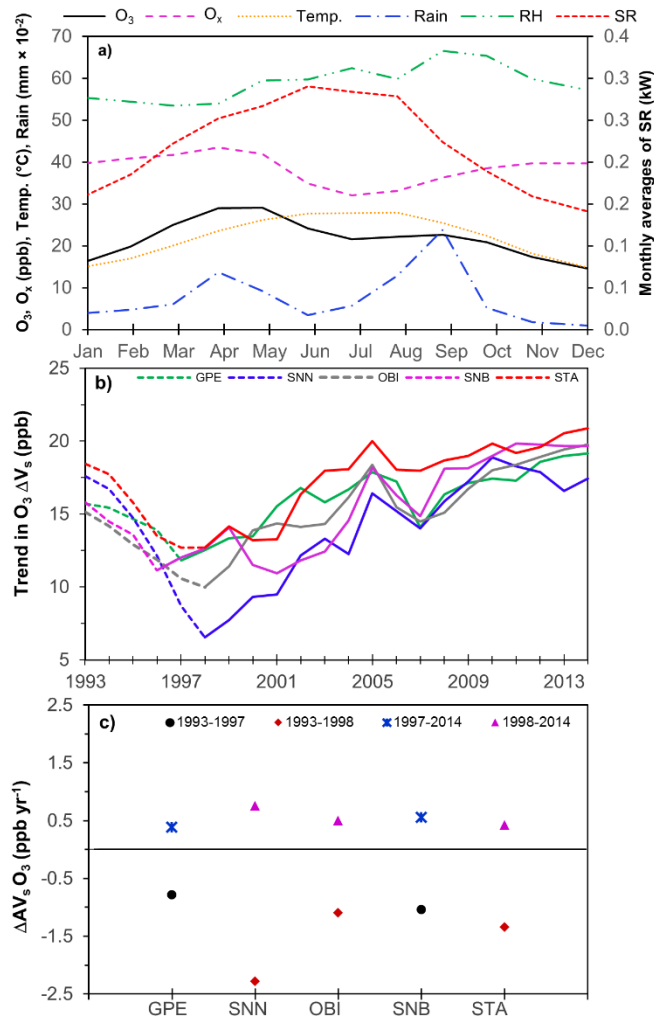


**Fig. 4.** Seasonal  $O_x$  de-trended daily profiles within the MMA during 1993-2014. De-trended  $O_x$  daily cycles were constructed by subtracting daily averages from hourly averages to remove the impact of long-term trends.



1084

1085

1086

1087

1088

1089

1090

**Fig. 5a).** Annual cycles of  $O_3$ , temperature, rainfall, RH and SR constructed by averaging records from 1993 to 2014 for a 1-year period. **b).** Trends in  $AV_s$  of  $O_3$  recorded at the 5 monitoring sites within the MMA from 1993 to 2014. The decline in  $AV_s$  observed is due to the economic crisis experienced in Mexico during 1994-1996, followed by persistent increases in  $AV_s$  since 1998. **c).** Annual rates of change in  $O_3$   $AV_s$  by site, before and after the 1994-1996 economic crisis.

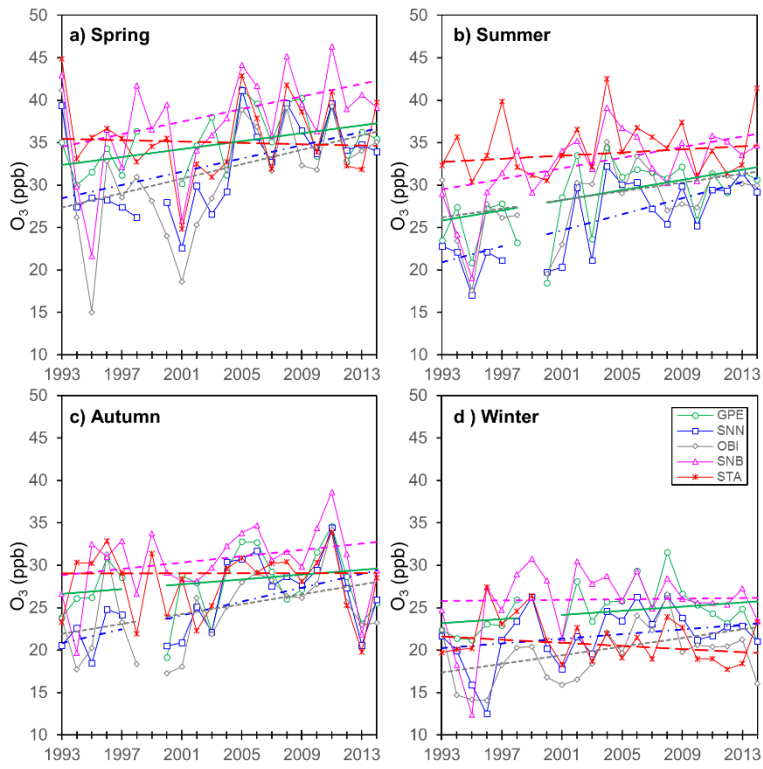


**Fig. 6.** Seasonal trends of  $O_3$  within the MMA during 1993-2014. Each data point represents the average of the 3-month period that defines the season. The continuous lines show the Sen trend.

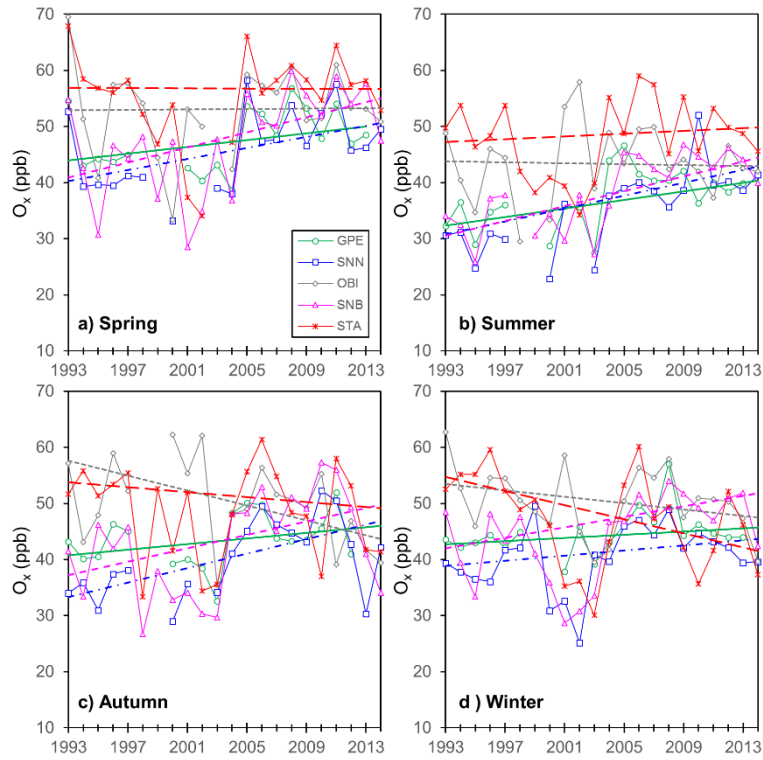
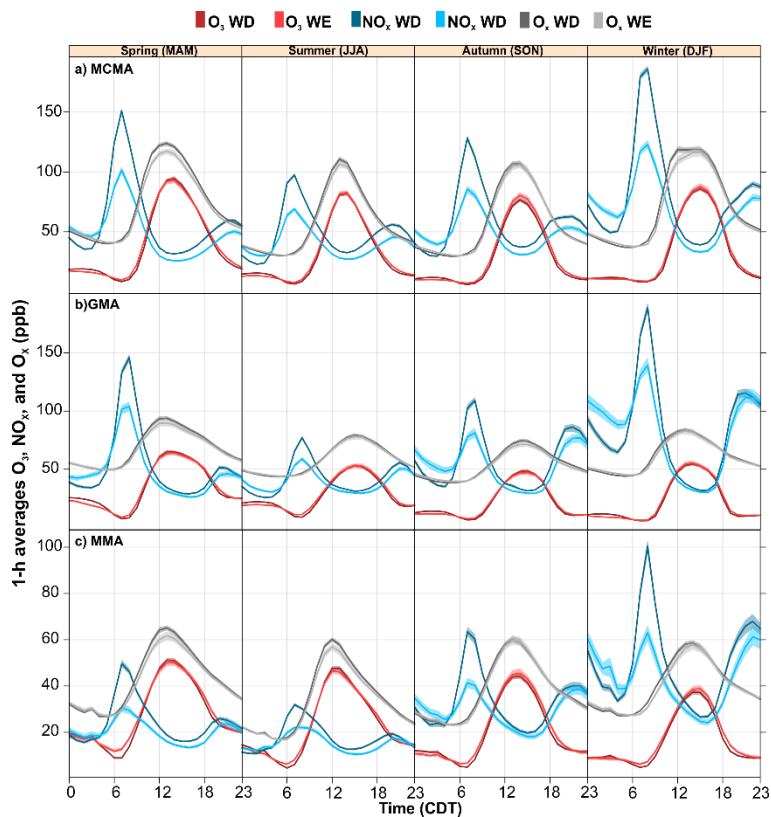
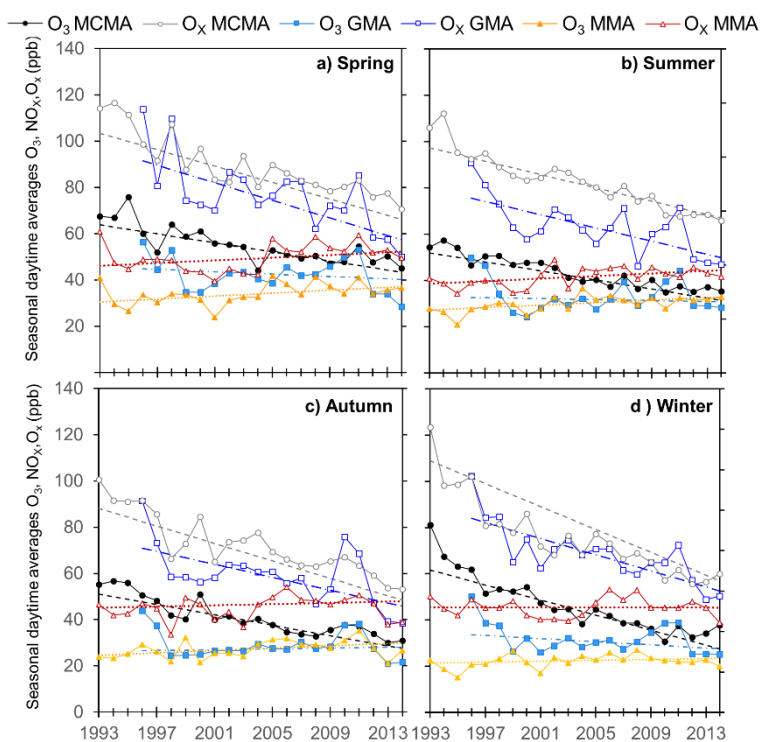


**Fig. 7.** Seasonal trends of  $O_x$  within the MMA during 1993-2014. Each data point represents the average of the 3-month period that defines the season. The continuous lines show the Sen trend.



1099  
1100  
1101  
1102  
1103  
1104

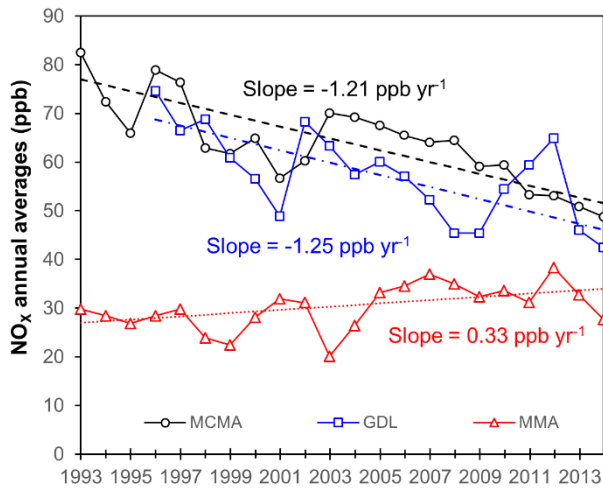
**Fig. 8.** Seasonal average diurnal cycles of  $O_3$ ,  $O_x$  and  $NO_x$  during 1993-2014 for the MCMA and the MMA, and between 1996-2014 for the GMA. The shading shows the 95% confidence intervals of the average, calculated through bootstrap resampling (Carslaw, 2015).



1105  
1106  
1107  
1108  
1109

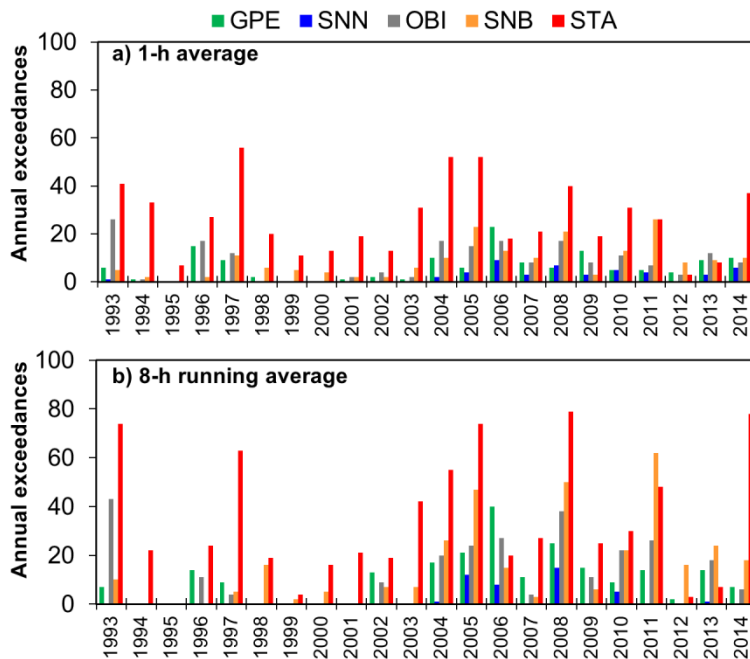
**Fig. 9.** Seasonal trends in  $O_3$  and  $O_x$  for the MCMA and MMA during 1993-2014, and for the GMA during 1996-2014. Each data point represents the average of the 3-month period that defines the season. The dashed lines show the Sen trend.





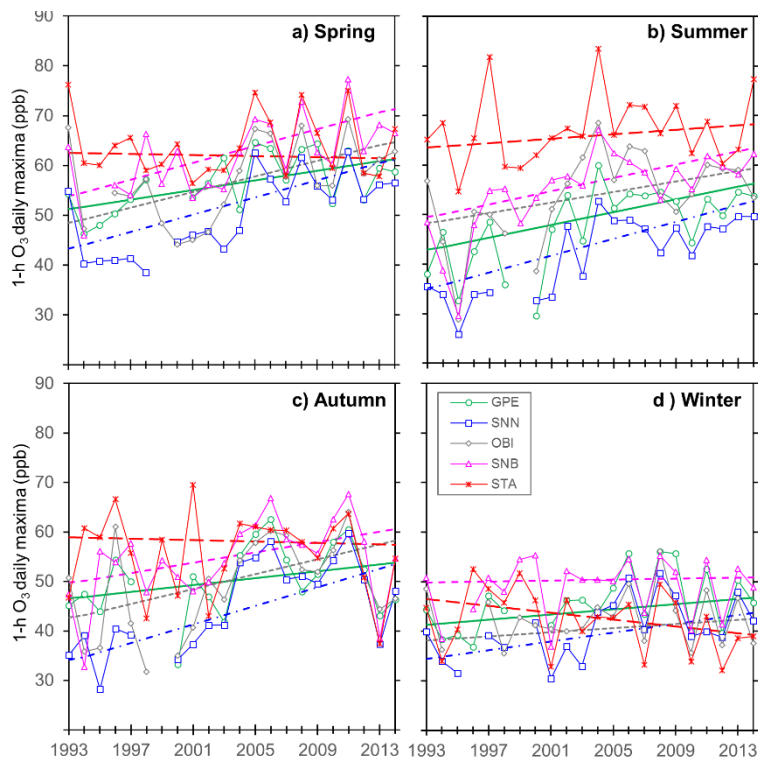
1110  
1111  
1112  
1113  
1114

**Fig. 10.** Trends for NO<sub>x</sub> at the MCMA and MMA during 1993-2014, and at the GMA during 1996-2014. The dashed lines represent the Sen slopes. All trends are statistically significant at  $p < 0.05$ .



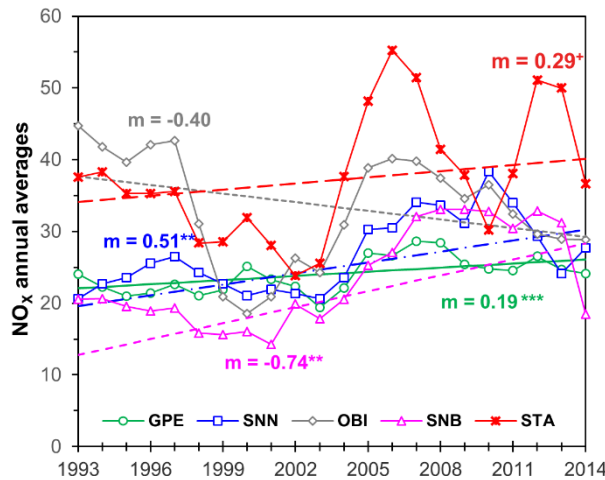
1115  
1116  
1117  
1118

**Fig. 11.** Annual exceedances of the O<sub>3</sub> NOM for 1-h averages (110 ppb) and 8-h running averages (80 ppb) at the 5 monitoring sites within the MMA from 1993 to 2014.



1119  
1120  
1121  
1122  
1123  
1124  
1125

**Fig. 12.** Seasonal trends in 1-h O<sub>3</sub> daily maxima at the MMA during 1993-2014. Each data point represents the average of the 3-month period that defines the season. The dashed lines show the Sen trend.



1126  
1127  
1128  
1129  
1130  
1131

**Fig. 13.** Long-term trends for NO<sub>x</sub> at the 5 monitoring sites within the MMA during 1993-2014. The dashed lines represent the Sen slopes. Annual NO<sub>x</sub> rates of change are described as  $m$  for slope and expressed in units of ppb yr<sup>-1</sup>. Levels of confidence are represented as  $+$  =  $p < 0.1$ ,  $*$  =  $p < 0.05$ ,  $**$  =  $p < 0.001$ ,  $***$  =  $p < 0.001$ .